

5-2016

## THE ROLE OF 5-ALPHA REDUCTASE 3 IN STEROID METABOLISM

zahi mitri

Follow this and additional works at: [https://digitalcommons.library.tmc.edu/utgsbs\\_dissertations](https://digitalcommons.library.tmc.edu/utgsbs_dissertations)

 Part of the [Endocrinology, Diabetes, and Metabolism Commons](#), and the [Oncology Commons](#)

---

### Recommended Citation

mitri, zahi, "THE ROLE OF 5-ALPHA REDUCTASE 3 IN STEROID METABOLISM" (2016). *The University of Texas MD Anderson Cancer Center UTHealth Graduate School of Biomedical Sciences Dissertations and Theses (Open Access)*. 661.

[https://digitalcommons.library.tmc.edu/utgsbs\\_dissertations/661](https://digitalcommons.library.tmc.edu/utgsbs_dissertations/661)

This Thesis (MS) is brought to you for free and open access by the The University of Texas MD Anderson Cancer Center UTHealth Graduate School of Biomedical Sciences at DigitalCommons@TMC. It has been accepted for inclusion in The University of Texas MD Anderson Cancer Center UTHealth Graduate School of Biomedical Sciences Dissertations and Theses (Open Access) by an authorized administrator of DigitalCommons@TMC. For more information, please contact [digitalcommons@library.tmc.edu](mailto:digitalcommons@library.tmc.edu).

THE ROLE OF 5-ALPHA REDUCTASE 3 IN STEROID METABOLISM

by

Zahi I Mitri, M.D.

APPROVED:

---

Mark Titus, Ph.D.  
Advisory Professor

---

Robert C Bast Jr, M.D.

---

David S Hong, M.D.

---

Filip Janku, M.D., Ph.D.

---

Jennifer K Litton, M.D.

APPROVED

---

Dean, The University of Texas

Graduate School of Biomedical Sciences at Houston

# THE ROLE OF 5-ALPHA REDUCTASE 3 IN STEROID METABOLISM

A

THESIS

Presented to the Faculty of

The University of Texas

Health Science Center at Houston

and

The University of Texas

MD Anderson Cancer Center

Graduate School of Biomedical Sciences

in Partial Fulfillment

of the Requirements

for the Degree of

MASTER OF SCIENCE

by

Zahi I Mitri, M.D.

Houston, Texas

May, 2016

## **Acknowledgements**

I would like to thank Dr. Mark Titus for being a phenomenal mentor and teacher over the past 2 years. I would like to thank Dr. Robert Bast, Dr. David Hong, Dr. Filip Janku, and Dr. Jennifer Litton for your mentorship and you agreeing to serve on my GSBS advisory committee. I really appreciate all the support, guidance and encouragement that you gave me to complete this degree. I would like to thank Dr. Gary Gallick for accepting to serve as a substitute member on my advisory committee for the thesis defense. I would like to thank Dr. Xin-Qiao Zhang for allowing me to use his laboratory space to complete this project when our lab was undergoing construction. I would like to extend a special thank you to Dr. Sumankalai Ramachandran, research investigator in Dr. Mark Titus' lab, for your patient from day one to teach me all the required laboratory and analytical skills required for the completion of the project. I could not have done this without Dr. Ramachandran's help and support. I would like to thank my hematology and medical oncology fellowship program director, Dr. Robert Wolff, for allowing me to enroll in the Master's program. I want to thank my wonderful wife, Souraya, and my beautiful daughter, Sophia, for their support and patience throughout my training.

## THE ROLE OF 5-ALPHA REDUCTASE 3 IN STEROID METABOLISM

Zahi I Mitri, M.D.

Advisor Professor: Mark Titus, Ph.D.

### **Background**

The growth and development of prostate cancer is largely driven by androgen mediated signaling. The 5-alpha reductase family of enzymes plays an essential role in the conversion of testosterone to the more potent androgen, 5-alpha dihydrotestosterone (DHT), which is capable of binding the androgen receptor to activate gene targets and downstream signaling. This study aimed to evaluate the role of 5-alpha reductase 3 (SRD5A3), a novel member of the 5-alpha reductase family, in steroid metabolism and prostate carcinogenesis.

### **Materials and Methods**

HEK293 cells were transfected with the SRD5A3 human cDNA ORF Clone from OriGene. Steroid substrates (testosterone, progesterone, androstenedione, epitestosterone, 11-ketotestosterone, 11 $\alpha$ -hydroxytestosterone, 11 $\beta$ -hydroxytestosterone, 6 $\beta$ -hydroxytestosterone, and cortisol) were added to transfected HEK293 cells. The dual 5-alpha reductase 1 and 2 inhibitor, dutasteride, was added to evaluate its inhibitory activity on SRD5A3 in the presence of each steroid. Mass spectrometry analysis was used to detect and quantify the conversion of steroid substrates to their 5-alpha reduced products.

### **Results**

SRD5A3 plasmid was successfully transfected into HEK293 cells. Mass spectrometry analysis confirmed that SRD5A3 converted testosterone to DHT. This reaction was completely inhibited

by dutasteride. SRD5A3 did not convert progesterone or androstenedione to the 5-alpha reduced products. SRD5A3 had the capacity of reducing testosterone derivatives to their 5-alpha reduced products. This catalysis was concentration dependent, with higher substrate levels yielding higher amounts of the 5-alpha reduced steroid product. The inhibitory activity of dutasteride on SRD5A3 was substrate and concentration dependent.

## **Conclusion**

SRD5A3 catalyzes the 5-alpha reduction of testosterone and testosterone analogues in the presence and absence of dutasteride. These 5-alpha reduced steroids are capable of binding and activating androgen receptor signaling. Further studies evaluating the role of SRD5A3 in prostate carcinogenesis are mandated to determine the role of therapeutic SRD5A3 inhibition across the spectrum of prostate cancer.

## Table of Contents

Approval Page.....	i
Title Page.....	ii
Acknowledgements.....	iii
Abstract.....	iv
Table of Contents.....	vi
List of illustrations.....	ix
List of tables.....	xi
Abbreviations.....	xii
 <b>Chapter 1: Background</b> .....	 1
 <b>Chapter 2: Materials and Methods</b> .....	 8
<i>2.1 Cell Culture</i> .....	9
<i>2.2 SRD5A3 Expression Vector</i> .....	11
<i>2.3 SRD5A3 Protein Expression - Creating a Transient Transfected Cell Line</i> .....	11
<i>2.4 SRD5A3 Protein Expression - Creating a Stable Transfected Cell Line</i> .....	12
<i>2.5 Immunoblot Analysis</i> .....	12

2.6 Protein Concentration.....	13
2.7 SRD5A3 Enzyme Assays.....	13
2.8 Mass Spectrometry Analysis.....	14
<b>Chapter 3: Results.....</b>	<b>17</b>
3.1 Cloning the SRD5A3 plasmid.....	18
3.2 SRD5A3 Transfection.....	20
3.3 Estimation of SRD5A3 Protein Concentration.....	22
3.4 Quantitative Mass Spectrometry.....	25
3.41 Testosterone.....	26
3.42 Progesterone.....	32
3.43 Androstenedione.....	34
3.44 Epitestosterone.....	36
3.45 6- $\beta$ -hydroxytestosterone.....	39
3.46 11- $\beta$ -hydroxytestosterone.....	42
3.47 11- $\alpha$ -hydroxytestosterone.....	45
3.48 11-ketotestosterone.....	48

<b>Chapter 4: Discussion.....</b>	<b>51</b>
<b>Chapter 5: Conclusion.....</b>	<b>58</b>
<b>Chapter 6: Limitations.....</b>	<b>60</b>
<b>Chapter 7: Bibliography.....</b>	<b>62</b>
<b>Vita.....</b>	<b>73</b>

## List of illustrations

Figure 1: HEK293 cell line growth time course.....	10
Figure 2: SRD5A3 Plasmid Sequence by PCR.....	19
Figure 3: SRD5A3 Immunoblot.....	21
Figure 4: Estimation of SRD5A3 Protein Concentration.....	23
Figure 5: Conversion of Testosterone to DHT by SRD5A3.....	27
Figure 6: DHT Standard Curve.....	28
Figure 7: Conversion of Testosterone to DHT by SRD5A3 Cell Lysate.....	29
Figure 8: Conversion of Testosterone to DHT with Addition of Dutasteride.....	30
Figure 9: SRD5A3 Protein Inhibition by Dutasteride.....	31
Figure 10: Conversion of Progesterone to Dihydroprogesterone by SRD5A3.....	33
Figure 11: Conversion of Androstenedione to Androstanedione by SRD5A3.....	35
Figure 12: 5- $\alpha$ Reduction of Epitestosterone by SRD5A3.....	37
Figure 13: SRD5A3 Protein Inhibition by Dutasteride – Epitestosterone.....	38
Figure 14: 5- $\alpha$ Reduction of 6- $\beta$ -hydroxytestosterone by SRD5A3.....	40
Figure 15: SRD5A3 Protein Inhibition by Dutasteride – 6- $\beta$ -hydroxytestosterone.....	41
Figure 16: 5- $\alpha$ Reduction of 11- $\beta$ -hydroxytestosterone by SRD5A3.....	43

Figure 17: SRD5A3 Protein Inhibition by Dutasteride – 11- $\beta$ -hydroxytestosterone.....	44
Figure 18: 5-alpha Reduction of 11- $\alpha$ -hydroxytestosterone by SRD5A3.....	46
Figure 19: SRD5A3 Protein Inhibition by Dutasteride – 11- $\alpha$ -hydroxytestosterone.....	47
Figure 20: 5-alpha Reduction of 11-ketotestosterone by SRD5A3.....	49
Figure 21: SRD5A3 Protein Inhibition by Dutasteride – 11-ketotestosterone.....	50

**List of tables**

Table 1: The increase in protein expression is measured by an increased in the optical density of the sample.....	24
---	----

**Abbreviations**

5-alpha dihydrotestosterone – DHT

Prostate Cancer Prevention Trial - PCPT

Reduction by Dutasteride of Prostate Cancer – REDUCE

5-alpha reductase-3 - SRD5A3

Dulbecco's Modified Eagle Medium – DMEM

Fetal Bovine Serum - FBS

Phosphate Buffered Saline – PBS

Luria Broth - LB Broth

Polymerase chain reaction – PCR

Sodium dodecyl sulfate – SDS

Tris-buffered saline with Tween - TBST

Liquid chromatography-mass spectrometry – LCMS

Standard - Std

## **CHAPTER 1: BACKGROUND**

The growth and development of prostate cancer is largely driven by androgen mediated signaling (1). Testosterone, the predominant circulating androgen, is produced in the testis under the control of luteinizing hormone. The 5-alpha reductase enzyme family plays a key role in the conversion of testosterone to the more potent androgen, 5-alpha dihydrotestosterone (DHT), in target organs such as the prostate (2). Given this pathophysiology, there has been interest in the development of 5-alpha reductase inhibitors for the treatment and prevention of prostate cancer. Two large trials have evaluated 5-alpha reductase inhibitors as chemoprevention for patients at high risk for developing prostate cancer. The Prostate Cancer Prevention Trial (PCPT) randomized >18,000 men to finasteride, a predominantly 5-alpha reductase 2 inhibitor, or placebo. The trial showed a decreased incidence of prostate cancer overall, but also a slight increase in the number of more aggressive tumors in the finasteride arm (3). One hypothesis to explain the increase in high-grade tumors in the finasteride arm is that this drug does not inhibit the 5-alpha reductase 1 enzyme. This isoform is overexpressed in prostate cancer, and has the ability to 5-alpha-reduce testosterone to DHT (4-7). In contrast, 5-alpha reductase 2 expression appears to either decrease or stay the same between normal prostate tissue and prostate cancer (5, 8). These observations led to the Reduction by Dutasteride of Prostate Cancer (REDUCE) trial. This study compared dutasteride, a dual 5-alpha reductase 1 and 2 inhibitor to placebo in men at high risk of developing prostate cancer. There was a significant reduction in the development of prostate cancer in this study, but again was noted a trend for developing high-grade prostate cancer in the control arm. This was lower than the risk previously observed in the finasteride prevention study (2, 9). Both clinical trials failed to show a mortality difference between the intervention and the placebo arms. Currently, 5-alpha reductase inhibitors are indicated for the treatment of benign prostate enlargement and lower urinary symptoms. Conversely, the use of

finasteride or dutasteride as chemoprevention remains controversial (10-14), and mainly based on a risk/benefit conversation between patients and their physicians.

In addition, 5-alpha reductase inhibitors have been evaluated in the treatment of prostate cancer (2, 14). Androgen deprivation therapy is the standard of care for advanced prostate cancer; however this therapy is not curative, with most tumors evolving into a castrate-resistant, also termed androgen-independent phenotype. Preclinical and clinical data have shown that the androgen receptor axis continues to be active under androgen deprivation therapy (15-18), and can potentially drive prostate cancer growth in an autocrine fashion (19-23). Androgen deprivation therapy achieves large reductions in systemic testosterone and DHT levels, however seems to have a lesser effect on testosterone and DHT levels within the prostate, where they remain at sufficient concentrations to activate the androgen receptor (22, 24-28). In addition, prostate cancer cells have the ability to use adrenal androgens such as dehydroepiandrosterone (DHEA) as substrates to produce testosterone and DHT and drive the androgen receptor (23, 28-31). The 5-alpha reductase enzyme family appears to continue to play a role in the production of DHT from steroid precursors in this setting, especially with data showing that 5-alpha reductase 1 and 5-alpha reductase-3 (*SRD5A3*) levels to be higher in prostate cancer compared to benign prostate tissue (4, 6-8). Furthermore, Li et al. demonstrated that activation of the androgen receptor negatively regulates *SRD5A3* expression by binding a negative androgen response element on the *SRD5A3* promoter (32). The reduction in androgen receptor expression in the setting of androgen deprivation therapy can then potentially lead to an increase in the expression of *SRD5A3*, and magnify its role in the production of DHT and tumor growth (32). 5-alpha reductase inhibitors either as single agent or in combination with androgen deprivation therapy or androgen receptor antagonists have been evaluated in several settings of prostate cancer

therapy (2). In the preoperative setting, the use of dutasteride before radical prostatectomy was associated with reduction in tumor volume and increased apoptosis (33, 34). The use of 5-alpha reductase inhibitors in the setting of biochemical relapse (35-37), castrate-sensitive (38-40), or castrate-resistant (41-43) advanced prostate cancer, has resulted in various levels of PSA decline, however no clinically meaningful survival endpoints have been reported to date. To date no clinical study has evaluated androgen deprivation therapy alone compared to androgen deprivation therapy combined with 5-alpha reductase inhibitors (2). More recently, the combination of dutasteride and enzalutamide, a novel androgen receptor antagonist, in the preclinical setting has shown to be synergistic in suppressing castrate-sensitive (LAPC4) and castrate-resistant (DuCaP) prostate cancer cell lines (44). Based on these preclinical and early phase studies, trials are planned to evaluate the role of 5-alpha reductase inhibitors in the management of prostate cancer. Currently, there are no data to support the use of 5-alpha reductase inhibitors for the treatment of prostate cancer (2, 14).

The development of prostate cancer despite 5-alpha reductase inhibition in the prevention setting, and that of castrate resistant prostate cancer despite androgen blockade raised the hypothesis of an alternate pathway of androgen production to drive carcinogenesis. More recently, a new 5-alpha reductase isoform, SRD5A3, was discovered. The first report by Uemura et al. in 2008 identified this novel gene using gene expression profiling in hormone refractory prostate cancer (5). The *SRD5A3* gene is located on the long (q) arm of chromosome 4 at position 12 (4q12) ([OMIM 611715](#)). This novel enzyme's sequence aligned with known sequences of 5-alpha reductase 1 and 5-alpha reductase 2, including conservation of the C-terminal domains, which are thought to be important in the catalytic activity of the 5-alpha reductase family in converting testosterone to DHT (5). Uemura et al. showed that SRD5A3 was

overexpressed in hormone refractory prostate cancer compared to hormone sensitive prostate cancer and normal prostate tissue. In contrast, 5-alpha reductase 2, the predominant isoform in the prostate, is overexpressed in the normal prostate and in hormone sensitive prostate cancer, and is almost absent in hormone refractory prostate cancer. The *SRD5A3* enzyme distribution was similar to 5-alpha reductase 1. In addition, the authors showed that *SRD5A3* had the ability to convert testosterone to DHT. In contrast, mutated *SRD5A3* lost its ability to reduce testosterone to DHT (5).

Despite this observation, much remained unknown about this new enzyme that appeared to loosely fit in the 5-alpha reductase family. In 2010, Cantagrel et al. evaluated a large consanguineous family where several children were born with ocular defects, brain malformations, heart defects and developmental delays (45). Genome-wide linkage analysis localized the mutations to the region of the *SRD5A3* gene, mutations that were not found in any of the unaffected control subjects. Interestingly, unlike defects in 5-alpha reductases 1 and 2, these children had no sexual development abnormalities ([OMIM #264600](#)) to suggest a defect in steroid hormone production. Given the clinical findings for these patients, further functional studies revealed that *SRD5A3* plays a role in N-linked glycosylation of surface proteins. *SRD5A3* encodes an enzyme that is required for the conversion of polyprenol to dolichol, an important molecule in the endoplasmic reticulum (45, 46). Following that, other reports linked congenital disorders of glycosylation with mutations in *SRD5A3*, with affected patients suffering from similar presentations, including cerebello-ocular syndromes. These studies showed that *SRD5A3* was expressed in the brain, heart and retina in normal human tissues, and significantly reduced in individuals with *SRD5A3* defects. This may explain the clinical manifestations in individuals carrying mutations in this enzyme (45, 47, 48).

Despite the discovery of a surprising role of *SRD5A3* in protein glycosylation, this enzyme's localization and role in prostate cancer remained a mystery. Two studies by Godoy and Yamana analyzed the distribution of *SRD5A3* in human tissues using immunohistochemical studies (49, 50). They found that *SRD5A3* was overexpressed in several androgen regulated (prostate, skeletal muscle, skin) and non androgen regulated (pancreas, colon, kidney) benign tissues. This observation supports that *SRD5A3* may play a role other than steroid reduction, potentially be involved in protein glycosylation as previously shown by Cantagrel et al. (45). Interestingly, *SRD5A3* was overexpressed in prostate cancer tissues compared to benign prostate tissue. This result aligns with the findings by Uemura et al., who had shown that the expression of *SRD5A3* seems to increase along prostate cancer carcinogenesis from benign tissue to castrate resistant cancer (5). With these findings regarding the localization of *SRD5A3*, Titus et al. evaluated *SRD5A3* function in castrate resistant prostate cancer specimen homogenates. Using clinical specimens, they first confirmed previous reports that *SRD5A3* was overexpressed in castrate resistant prostate cancer compared to 5-alpha reductase 1 and 5-alpha reductase 2 (51). In addition, Titus et al. expressed a HP-Thioredoxin-fusion *SRD5A3* protein using a pBAD/Thio-TOPO vector in CHO-K1 cells (mammalian system), and TOP10 *E.coli* competent cells. The HP-Thioredoxin-fusion *SRD5A3* protein in both systems was found to be catalytically active and 5 $\alpha$ -reduced testosterone to DHT. However 5 $\alpha$ -reduced steroids were produced in low amounts. This reaction was partially inhibited by dutasteride or abiraterone, suggesting that *SRD5A3* can sustain DHT formation even in the presence of 5-alpha reductase 1 and 2 inhibitors, and potentially sustain prostate cancer development. Of note, this fusion protein also converted androstenedione and progesterone to their 5 $\alpha$ -reduced products, androstenedione and dihydroprogesterone (51).

In contrast to these findings, a recent report looking at both hamster and human SRD5A3 showed that the enzyme was unable to reduce testosterone to DHT (52). In this study, Chaves et al. evaluated the 5-alpha reducing capacity of hamster SRD5A3 expressed as a fusion protein with green fluorescent protein from the pcDNA3.1-NT-GFP/hSrd5a3 plasmid and human SRD5A3 (OriGene, Maryland, USA) (52). Of note, the fusion protein localized to the cytoplasm, whereas the SRD5A3 enzyme has been described to be a membrane protein involved in protein glycosylation (45).

Several reports have now been published on SRD5A3; however its role in the pathogenesis of prostate cancer and in steroid metabolism has not been clearly defined. SRD5A3 is ubiquitously expressed in human tissues –both benign and malignant- and plays a role in N-linked protein glycosylation (45); with defects in this enzyme having been linked with congenital disorders of glycosylation (45, 47, 48). This study aims to evaluate the role of SRD5A3 in steroid metabolism, and elucidate its role in prostate carcinogenesis. Specifically, this study first assessed the ability of SRD5A3 to convert steroid precursors to their 5-alpha reduced products. Additionally, the effect of dutasteride on SRD5A3 function was also evaluated for each steroid precursor.

## **CHAPTER 2: MATERIALS AND METHODS**

## ***2.1 Cell Culture***

The HEK293 cell line (cat# CRL-1573, ATCC, VA, USA) was used in this experiment. This is a permanent cell line established from primary embryonic human kidney and transformed with human adenovirus type 5 DNA (<http://www.atcc.org/products/all/VR-1516.aspx>). The E1A adenovirus gene is expressed in these cells and participates in transactivation of some viral promoters, allowing these cells to produce very high levels of protein. HEK293 cells were prepared from a clone selected for fast growth in serum-free medium (Figure 1), good adherence during plaque assays, superior transfection efficiencies and a high level of protein expression.

HEK293 cells that had been frozen in liquid nitrogen were removed and thawed on ice. When thawed, cells were added to a 10 cm plate containing 10 mL of Dulbecco's Modified Eagle Medium (DMEM) (cat # SH30022.01, HyClone, Utah, USA) to which were added 10% Fetal Bovine Serum (FBS) (cat #10437-077, Thermo Fisher Scientific, Massachusetts, USA) and Antibiotic-Antimycotic (cat # 15240-062, Thermo Fisher Scientific, Massachusetts, USA). Plates become confluent and ready to split within 24-48 hours. To split HEK293 cells, media was removed and the cells were washed with Phosphate Buffered Saline (PBS). After that, trypsin (cat # 25-053-CI, Corning, VA, USA) was added to the plate and the cells were placed in the incubator for 2-3 minutes. Plates were removed and the cells observed to ensure they have detached. At that point, DMEM was added to neutralize the trypsin effect. The cells were then aliquoted into the desired number of plates, and to each plate was added DMEM to a total volume of 10 mL.

Figure 1. HEK293 cell line growth time course

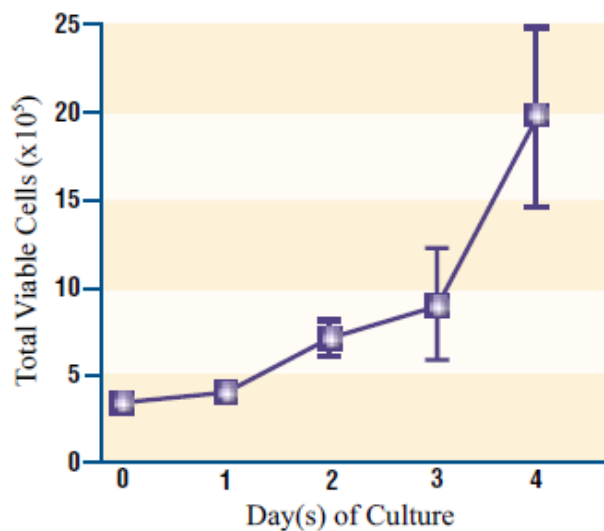


**Figure 1. The average HEK-293 cell doubling time in shaker flask.** HEK293 suspension cells were seeded at  $3 \times 10^5$  cells/mL in 125 mL shaker flasks containing 20 mL media. Results show average doubling time of 33 hours and average density approaching  $2 \times 10^6$  cells/mL over a period of four days.

## ***2.2 SRD5A3 Expression Vector***

DH5 $\alpha$  E.coli competent cells were used to clone the SRD5A3 vector using a heat shock protocol. The SRD5A3 vector was diluted to 10 ng/ $\mu$ L, and then 2  $\mu$ L were added to 4 tubes containing 45  $\mu$ L DH5 $\alpha$  cells. The cells were incubated on ice for 30 minutes, and then exposed to a heat shock for 20 seconds in a 42°C water bath without shaking. The cells were then placed on ice for 2 minutes. Pre-warmed Luria Broth (LB Broth) was added to each tube and incubated at 37°C for 1 hour in a heated shaker at 225 rpm. Next, 20 to 200  $\mu$ L of broth from each tube were added to LB plates and incubated overnight at 37°C. Subsequently, I picked bacterial colonies and inoculated LB broth. The SRD5A3 vector was isolated from E.coli and polymerase chain reaction (PCR) confirmed that the cDNA sequence matched the published sequence of the SRD5A3. Four different colonies were picked and the vector was quantified (ranged from 200-500  $\mu$ g of DNA).

## ***2.3 SRD5A3 Protein Expression - Creating a Transient Transfected Cell Line***

The transfection experiment was run using the SRD5A3 ([NM\\_024592](#)) human cDNA ORF Clone from OriGene (cat # RC200970, Maryland, USA). HEK293 cells were plated until they achieved 60-70% confluency in 10 cm plates. The OriGene application guide protocol for transient transfection was implemented during this experiment. Opti-Minimal Essential Medium (MEM, cat# 51985091, Thermo Fisher Scientific, Massachusetts, USA) 1.0 mL was added to each 10 cm plate. 10  $\mu$ g of DNA was added to each plate as recommended by application guide (5-25  $\mu$ g DNA per 10 cm plate), and then Turbofectin (cat# TF81001, OriGene, Maryland, USA) was added in a ratio of 3:1 (Turbofectin: DNA). The cells were then incubated for 30 minutes at room temperature. Following that, 9 mL of DMEM were added to the plates.

## ***2.4 SRD5A3 Protein Expression - Creating a Stable Transfected Cell Line***

Using a transiently transfected plate 24 hours after transfection, cells were passaged into fresh growth medium with the selective agent and Antibiotic-Antimycotic. After passaging the cells and adding fresh medium to allow for growth, in the presence of the selective agent, immunoblot analysis was performed to confirm that the cells continued to harbor the transfected plasmid. This process aimed to generate a stably transfected HEK293 cell line for future experiments.

## ***2.5 Immunoblot Analysis***

Acrylamide gels (12%) were prepared using the following reagents: water, 30% acrylamide mix (cat # 161-0158, Bio-Rad, California, USA), 1.5M Tris buffer (pH 8.8) (cat # 161-0798, Bio-Rad, California, USA), 10% sodium dodecyl sulfate (SDS) solution (cat # 161-0416, Bio-Rad, California, USA), 10% Ammonium Per sulfate (cat # 161-0700, Bio-Rad, California, USA), and TEMED (cat # 161-0800, Bio-Rad, California, USA). The lanes of each stacking gel were loaded with: molecular weight markers, negative control (cells without vector), and positive control (cat# RC200970, OriGene, Maryland, USA), positive control (cloned vector), and positive protein lysate (OriGene). The samples were run on the gel at 100 volts for 2 hours. Then, the separated proteins were transferred onto nitrocellulose for 2 hours. The nitrocellulose was removed from the transfer apparatus and immunoblot was performed using primary antibodies to DDK epitope (cat# AR100023, OriGene, Maryland, USA), SRD5A3 (cat# PA5-25200, Thermo Fisher Scientific, Massachusetts, USA), and actin (cat# ab8229, Abcam, Massachusetts, USA). Immunoblots were performed as described below:

1. The nitrocellulose was blocked for 30 minutes in 5% milk

2. Two washes in 10 mL Tris-buffered saline with Tween (TBST), 10 minutes each
3. Incubation with actin (3  $\mu$ L in 5.0 mL BSA) and DDK (3  $\mu$ L in 5.0 mL BSA) primary antibodies
4. Four washes in 10 mL TBST, 10 minutes each
5. A second block was applied using 5% milk in TBST for 30 minutes
6. Two washes with 10 mL TBST, 10 minutes each
7. Secondary antibody (3  $\mu$ L in 5 mL of 3% BSA) for 45 minutes
8. Four washes with 10 mL TBST, 10 minutes each
9. The nitrocellulose was exposed for 2 minutes and developed in the dark room.

## ***2.6 Protein Concentration***

The optimal timing of protein expression following transfection was determined by quantifying amount of total cell protein (Bradford Protein Assay Kit, Bio-Rad (product #23208, Bio-Rad, CA, USA)) using lysates from fixed time intervals. The results were graphed to determine the time point of maximum protein expression.

## ***2.7 SRD5A3 Enzyme Assays***

The stably transfected HEK293 cell line was used to determine the enzymatic function of the SRD5A3 vector with the addition of the following C-13 labeled steroid compounds:

- Testosterone ([cat# T1500, Sigma-Aldrich, Missouri, USA](#)),
- Progesterone ([cat# 10314, IsoSciences, Pennsylvania, USA](#)),
- Dihydrotestosterone ([cat# 6065, IsoSciences, Pennsylvania, USA](#)),

- Androstenedione ([cat# 9044, IsoSciences, Pennsylvania, USA](#)),
- Epitestosterone ([cat# E5878, Sigma-Aldrich, Missouri, USA](#)),
- 11 $\alpha$ -hydroxytestosterone ([cat# 10008647, Cayman Chemicals, Michigan, USA](#)),
- 6 $\beta$ -hydroxytestosterone ([cat# H2898, Sigma-Aldrich, Missouri, USA](#)),
- 11 $\beta$ -hydroxytestosterone ([cat# A5760-000, Steraloids, Rhode Island, USA](#)),
- 11-ketotestosterone ([cat# A6720-000, Steraloids, Rhode Island, USA](#)), and
- Cortisol ([cat# 14465 IsoSciences, Pennsylvania, USA](#)).

Each test steroid was added to DMEM containing 10% charcoal-stripped Fetal Bovine Serum (cat# F6765, Sigma-Aldrich, Missouri, USA) and Antibiotic-Antimycotic. Most endogenous steroids have been removed hence the effect of added steroids is monitored in the experiments. At 48 hours, the cell pellets and media were collected for steroid analysis using quantitative mass spectrometry.

## ***2.8 Mass Spectrometry Analysis***

Mass spectrometry analysis was performed using an Agilent 1290 UHPLC system (Agilent Infinity 1290 Autosampler, Binary Pump, Thermostatted Column Compartment), coupled to an Agilent 6490 Mass Spectrometer with Jet Stream Technology ESI source. Separation was achieved using a Chromolith Fast Gradient chromatography column, RP-18e, 50 x 2mm, 1.5  $\mu$ m particle size. The analysis was done using the MassHunter Workstation Quantitative Analysis Software (Version B.06.00 SP01/Build 6.0.388.1, Agilent, California, USA).

Cell pellets were reconstituted in 200  $\mu$ L of UHPLC grade water and then spiked with 10  $\mu$ L of a 10ng/mL C-13 steroid internal standard solution (C-13 Testosterone, C-13 Progesterone

and C-13 DHT, C-13 Pregnenolone). Media (200  $\mu$ L) was also aliquoted and spiked with 10  $\mu$ L of a 10ng/mL internal standard solution. Methyl t-butyl ether (MTBE) (3.0 ml) was then added and the sample was extracted with rocking for 15 minutes at room temperature. The organic layer was then separated by centrifugation, decanted and evaporated down to dryness under a steady stream of medical grade nitrogen. The residue was then reconstituted in 100  $\mu$ L methanol. An aliquot (100  $\mu$ L) of 1.5M Hydroxylamine hydrochloride (cat# 159417, Sigma-Aldrich, Missouri, USA) was then added and the mixture was heated at 65°C for 60 minutes. The samples were then transferred into liquid chromatography-mass spectrometry (LCMS) vials and analyzed by triple quadrupole mass spectrometry.

In addition, an 8 point standard (Std) calibration curve for the following 11 androgens was analyzed using mass spectrometry:

- Testosterone = 1.0 to 1000 pg/mL
- Epitestosterone = 1.0 to 1000 pg/mL
- Androstenedione = 1.0 to 1000 pg/mL
- Dihydrotestosterone = 10 to 1000 pg/mL
- Progesterone = 1.0 to 1000 pg/mL
- Dihydroprogesterone = 50 to 1000 pg/mL ([cat# P2750-000, Steraloids, Rhode Island, USA](#))
- Pregnenolone = 10 to 1000 pg/mL ([cat# Q5500-000, Steraloids, Rhode Island, USA](#))
- 17-hydroxyprogesterone = 1.0 to 1000 pg/mL ([cat# Q3360-000, Steraloids, Rhode Island, USA](#))
- Cortisol = 10 to 1000 pg/mL
- Androstenedione = 10 to 1000 pg/mL ([cat# A1630-000, Steraloids, Rhode Island, USA](#))

- [5-alpha pregnan-3-ol-20-one](#) = 10 to 1000 pg/mL ([cat# P3830-000, Steraloids, Rhode Island, USA](#))

This was done using the following stock solutions in methanol: Std1: 0.02 ng/mL (1 pg/mL); Std2: 0.1 ng/mL (5 pg/mL); Std3: 0.2 ng/mL (10 pg/mL) Std4: 1 ng/mL (50 pg/mL); Std5: 2 ng/mL (100 pg/mL); Std6: 5 ng/mL (250 pg/mL); Std7: 10 ng/mL (500 pg/mL); Std8: 20 ng/mL (1000 pg/mL). Two quality control (QC) solutions (representing both high and low concentrations) were also prepared using the following two solutions: QC1: 0.4 ng/mL (20 pg/mL); QC2: 15 ng/mL (750 pg/mL). The standard curve and QC samples were prepared with the same method used for sample extraction detailed above.

## **CHAPTER 3: RESULTS**

### ***3.1 Cloning the SRD5A3 plasmid***

The SRD5A3 vector was successfully cloned in DH5 $\alpha$  E.coli competent cells. PCR was used to confirm that our results matched the published sequence of the SRD5A3 vector with 98% concordance (Figure 2). Four colonies were obtained, yielding 496.4  $\mu$ g, 266  $\mu$ g, 466  $\mu$ g, and 510  $\mu$ g of vector respectively.

Figure 2. SRD5A3 Plasmid Sequence by PCR

Score	Expect	Identities	Gaps	Strand
1393 bits(1544)	0.0	805/821(98%)	8/821(0%)	Plus/Plus
Query 1	ATGGCTCCCTGGGCGGAGGCCGAGCACTCGGCGCTGAACCCGCTGCGCGGGTGTGGCTC	60		
Sbjct 150	ATGGCTCCCTGGGCGGAGGCCGAGCACTCGGCGCTGAACCCGCTGCGCGGGTGTGGCTC	209		
Query 61	ACGCTGACCGCCGCTTCTGCTGACCCTACTGCTGCAGCTCCTGCCGCCCGGCTGCTC	120		
Sbjct 210	ACGCTGACCGCCGCTTCTGCTGACCCTACTGCTGCAGCTCCTGCCGCCCGGCTGCTC	269		
Query 121	CCGGGCTGCGCGATCTTCCAGGACCTGATCCGCTATGGGAAAACCAAGTGTGGGGAGCCG	180		
Sbjct 270	CCGGGCTGCGCGATCTTCCAGGACCTGATCCGCTATGGGAAAACCAAGTGTGGGGAGCCG	329		
Query 181	TCGCGCCCCGCCGCTGCCGAGCCTTTGATGTCCCAAGAGATATTTTCCCACTTTTAT	240		
Sbjct 330	TCGCGCCCCGCCGCTGCCGAGCCTTTGATGTCCCAAGAGATATTTTCCCACTTTTAT	389		
Query 241	ATCATCTCAGTGCTGTGGAATGGCTTCTGCTTTGGTGCCTTACTCAATCTCTGTTCTTG	300		
Sbjct 390	ATCATCTCAGTGCTGTGGAATGGCTTCTGCTTTGGTGCCTTACTCAATCTCTGTTCTTG	449		
Query 301	GGAGCACCTTTTCCAAGCTGGCTTCATGGTTTGCTCAGAATTCTCGGGGCGGCACAGTTC	360		
Sbjct 450	GGAGCACCTTTTCCAAGCTGGCTTCATGGTTTGCTCAGAATTCTCGGGGCGGCACAGTTC	509		
Query 361	CAGGGAGGGGAGCTGGCACTGTCTGCATTCTAGTGCTAGTATTTCTGTGGCTGCACAGC	420		
Sbjct 510	CAGGGAGGGGAGCTGGCACTGTCTGCATTCTAGTGCTAGTATTTCTGTGGCTGCACAGC	569		
Query 421	TTACGAAGACTCTTCGAGTGCCCTACGTCACTGCTTCTCCAATGTCATGATTCACGTC	480		
Sbjct 570	TTACGAAGACTCTTCGAGTGCCCTACGTCACTGCTTCTCCAATGTCATGATTCACGTC	629		
Query 481	GTGCACTACTGTTTTGGACTTGCTATTATGTCCTTGTGGCCTAACTGTGCTGAGCCAA	540		
Sbjct 630	GTGCACTACTGTTTTGGACTTGCTATTATGTCCTTGTGGCCTAACTGTGCTGAGCCAA	689		
Query 541	GTGCCAATGGATGGCAGGAATGCCTACATAACAGGGAAAAATCTATTGATGCAAGCACGG	600		
Sbjct 690	GTGCCAATGGATGGCAGGAATGCCTACATAACAGGGAAAAATCTATTGATGCAAGCACGG	749		
Query 601	TGGTTCCATATTCTTGGGATGATGATGTTTCATCTGGTCATCTGCCCATCAGTATAAGTGC	660		
Sbjct 750	TGGTTCCATATTCTTGGGATGATGATGTTTCATCTGGTCATCTGCCCATCAGTATAAGTGC	809		
Query 661	CATGTTATTCTCGGCAATCTCAGGAAAAATAAGCAGGAGTGGTCA-TTCACTGTAACCA	719		
Sbjct 810	CATGTTATTCTCGGCAATCTCAGGAAAAATAAGCAGGAGTGGTCA-TTCACTGTAACCA	869		
Query 720	CAGGATCCCATTTGG-AGACTGGTTTG--AATATGTTTC-TTCCCCTAACTACTTAGCAG	775		
Sbjct 870	CANGATCCCATTTGGAAGACTGGNTTNGAAATATGTTTCTTCCCCTAACTACTTAGCAA	929		
Query 776	AGCTGATGATCTACGTTT--CCATGGCCGTC-ACCTTTGGG	813		
Sbjct 930	ANCTGATGATCTACGTTTCCAAGGGCCGTCAACCTTTNGG	970		

Figure 2. PCR sequence of the cloned *SRD5A3* plasmid matched with the published sequence of *SRD5A3*

### 3.2 *SRD5A3* Transfection

The HEK293 cells were initially transfected with the generated *SRD5A3* expression vector. Immunoblot analysis was performed using anti-DDK, anti-*SRD5A3* and anti-actin antibodies. The results confirmed the presence of the *SRD5A3* protein band at 37 kDa using the anti-DDK antibody. However, no band was detected on the immunoblot using the anti-*SRD5A3* antibody. The immunoblot was repeated by adding increasing amounts of protein lysates to successive wells. Using the anti-DDK antibody, the immunoblot results showed that with increasing amounts of material, there is a commensurate increase in the size of the 37 kDa band corresponding to the *SRD5A3* protein (Figure 3). Following confirmation of the transient transfection of the *SRD5A3* vector, HEK293 cells underwent a stable transfection protocol. The integration of the *SRD5A3* vector in these stably transfected cells was confirmed by immunoblot.

**Figure 3. SRD5A3 Immunoblot**

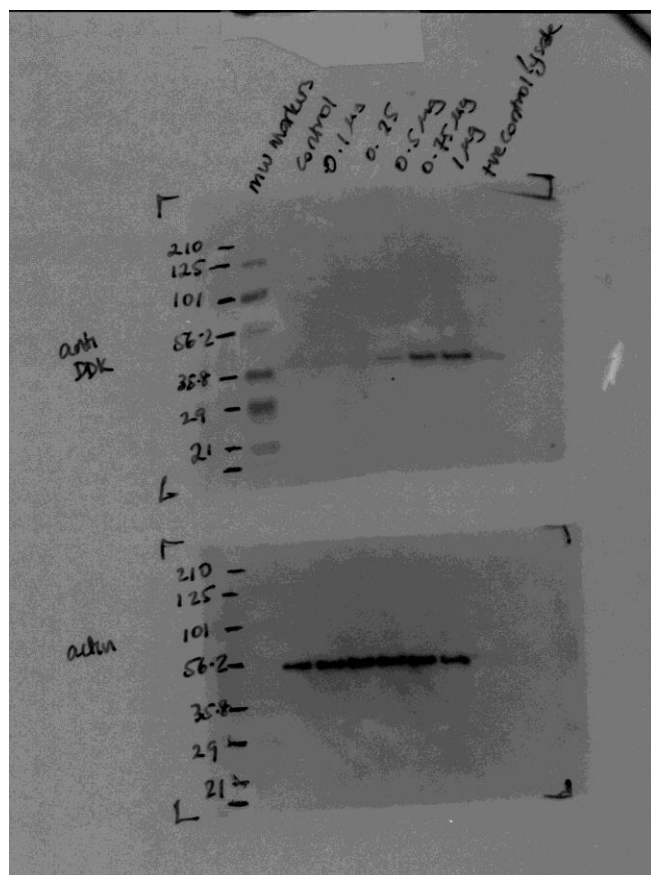


Figure 3. Immunoblot using anti-DDK antibody to detect the SRD5A3 protein. There is an increase in the size of the 37kDa band corresponding to SRD5A3 with increasing amounts of protein lysate loaded into the wells (Top panel). Actin control for the immunoblot (Bottom panel).

### ***3.3 Estimation of SRD5A3 Protein Concentration***

The amount of SRD5A3 present in transfection was evaluated at successive intervals following transfection. There was an increase in the optical density, and subsequently of the protein expression in the system over the first 72 hours, after which the expression started decreasing. The time point of 72 hours post transfection was identified to correspond to the highest SRD5A3 protein expression (Figure 4). This time point was used for all experiments to evaluate the enzymatic activity of SRD5A3 in steroid metabolism.

**Figure 4. Estimation of SRD5A3 Protein Concentration**

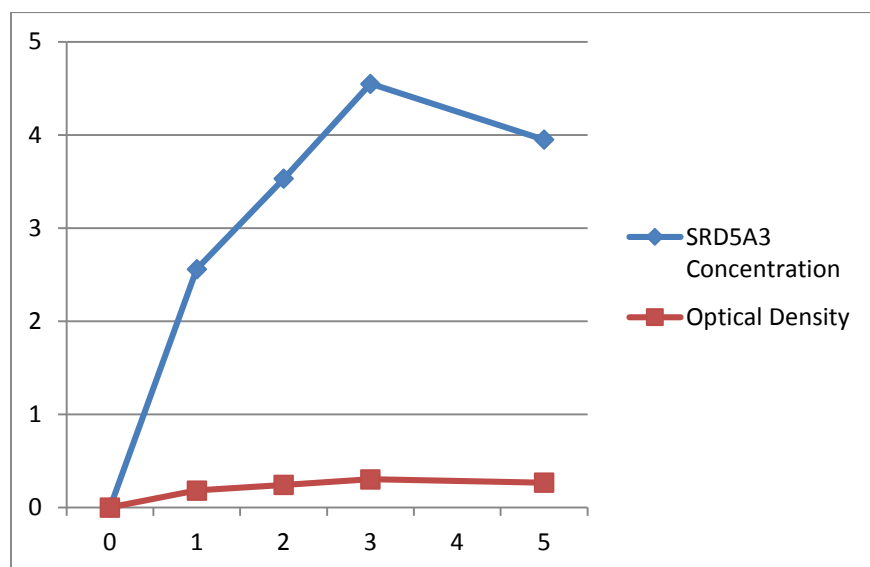


Figure 4. SRD5A3 protein concentration shows increasing protein expression after transfection (D0) that peaks around day 3.

**Table 1. The increase in protein expression is measured by an increased in the optical density of the sample**

<b>DAY</b>	<b>OPTICAL DENSITY</b>	<b>CONCENTRATION (<math>\mu\text{g}/\mu\text{l}</math>)</b>
0	0	0
1	0.182	2.561
2	0.242	3.532
3	0.302	4.55
4	N/A	N/A
5	0.267	3.95

### ***3.4 Quantitative Mass Spectrometry***

Liquid chromatography mass spectrometry analysis was used to determine the presence or absence of reduced products following the addition of C-13 labeled precursor steroids to HEK293 cells transfected with the SRD5A3 vector. Dutasteride, a known 5-alpha reductase 1 and 2 inhibitor, was added to each steroid precursor to determine its effect on the enzymatic activity of SRD5A3.

### 3.41. Testosterone

C-13 labeled testosterone at 1 and 10  $\mu$ M was added to HEK293 control cells (non-transfected) and HEK293 transfected cells. C-13 labeled testosterone was converted to DHT only in the transfected system (Figure 5). Notably, the baseline steroid profile of non-transfected HEK293 cells without the addition of any steroids did not contain any DHT.

In addition, a standard curve for DHT using C-13 internal standards was created to quantify the amount of DHT produced following the addition of testosterone (Figure 6). The amount of DHT produced was quantified by mass spectrometry and showed a positive correlation with the amount of precursor C-13 labeled testosterone introduced. The addition of 1  $\mu$ M C-13 labeled testosterone yielded 379.7  $\pm$  19.4 pg/mL of DHT; 10  $\mu$ M C-13 labeled testosterone yielded 2129.7  $\pm$  177.4 pg/mL of DHT. These findings confirmed that the SRD5A3 enzyme catalyzes the conversion of testosterone to DHT.

Furthermore, we generated a cell free lysate of the HEK293 transfected cells, to which we added C-13 labeled testosterone. In this setting, we did not detect evidence of conversion of C-13 labeled testosterone to DHT by mass spectrometry (Figure 7).

The addition of 1 nM dutasteride completely inhibited the conversion of C-13 labeled testosterone to DHT. DHT was not detected by mass spectrometry following the addition of 1  $\mu$ M or 10  $\mu$ M of C-13 labeled testosterone (Figures 8, 9).

**Figure 5. Conversion of Testosterone to DHT by SRD5A3**

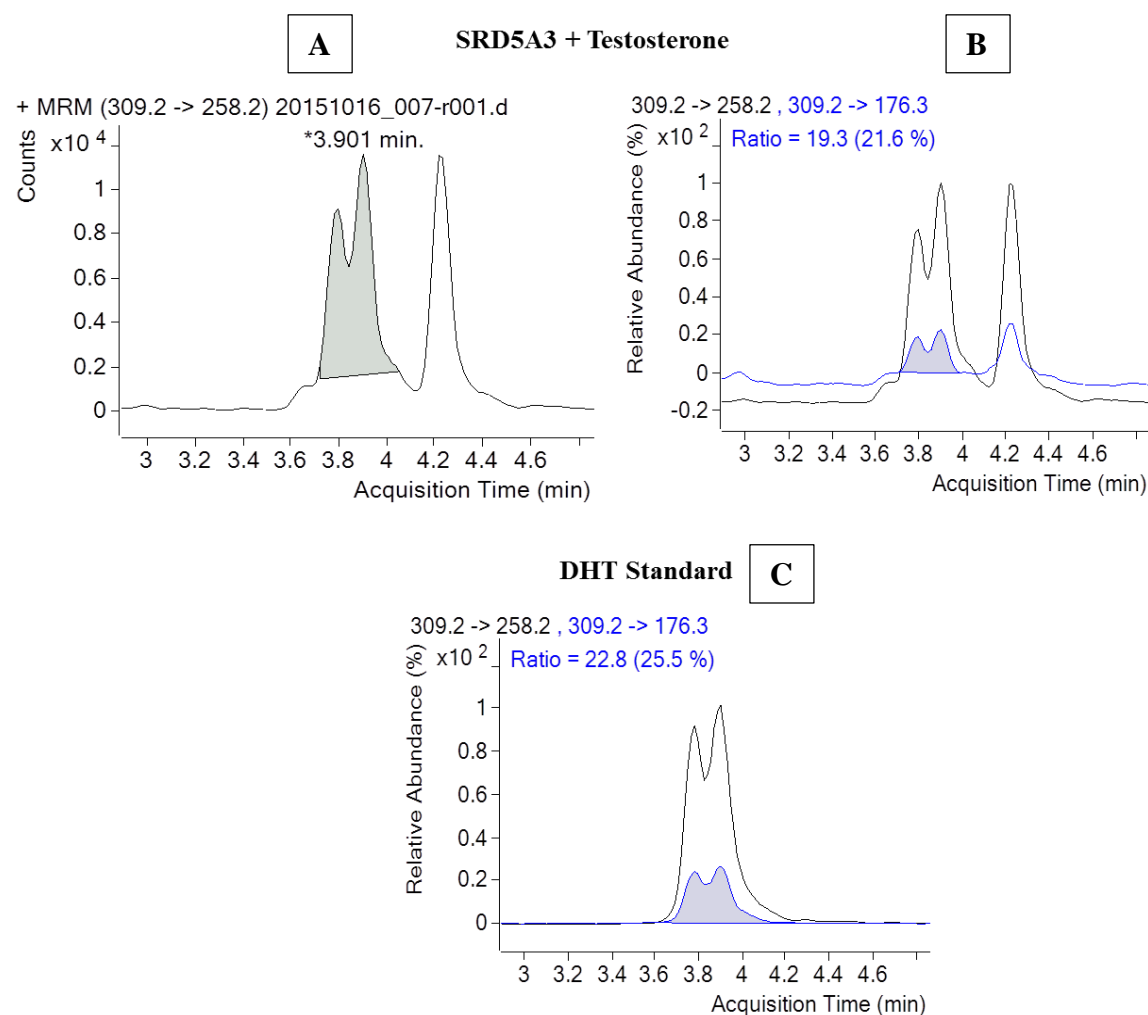


Figure 5. HEK293 cells transfected with SRD5A3 vector reduced testosterone to DHT. Testosterone added to HEK293 cells showed that DHT was detected and quantified using mass spectrometry. The double peak eluting at 3.901 minutes (Panel A) was fragmented into a qualifier and quantifier ion (Panel B). The DHT retention time, ratio of qualifier/quantifier ion corresponds to results obtained with the DHT internal standard (Panel C).

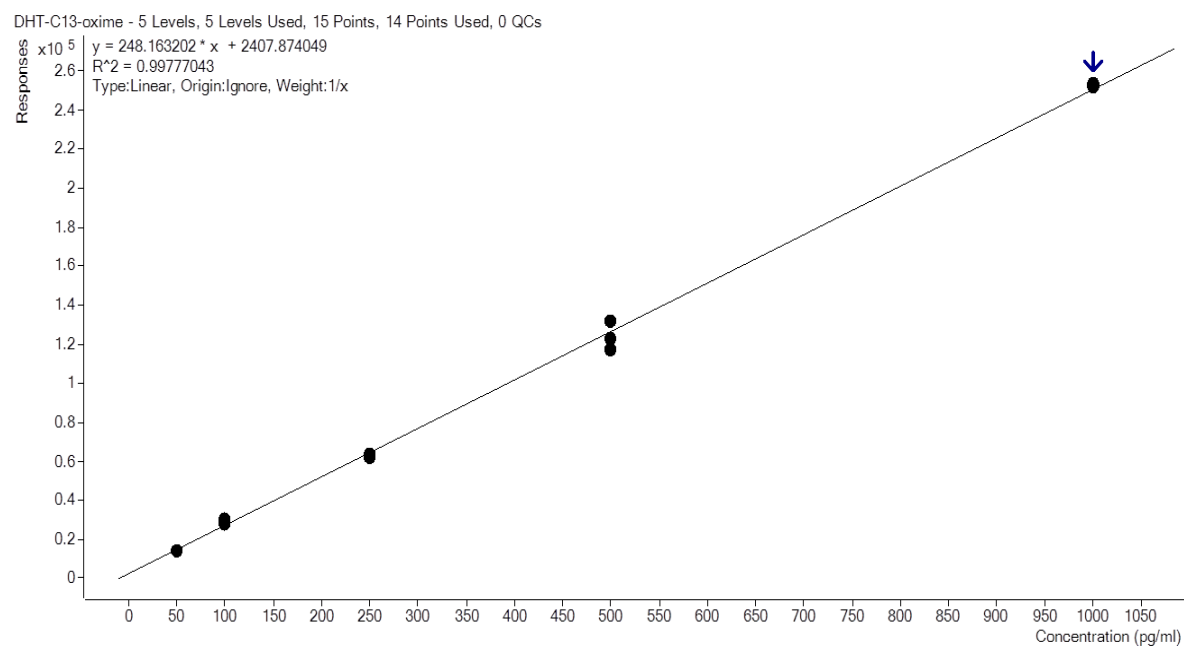
**Figure 6. DHT Standard Curve**

Figure 6. DHT standard curve was created using the following DHT concentrations: 50, 100, 250, 500, and 1000 pg/mL.

**Figure 7. Conversion of Testosterone to DHT by SRD5A3 Cell Lysate**

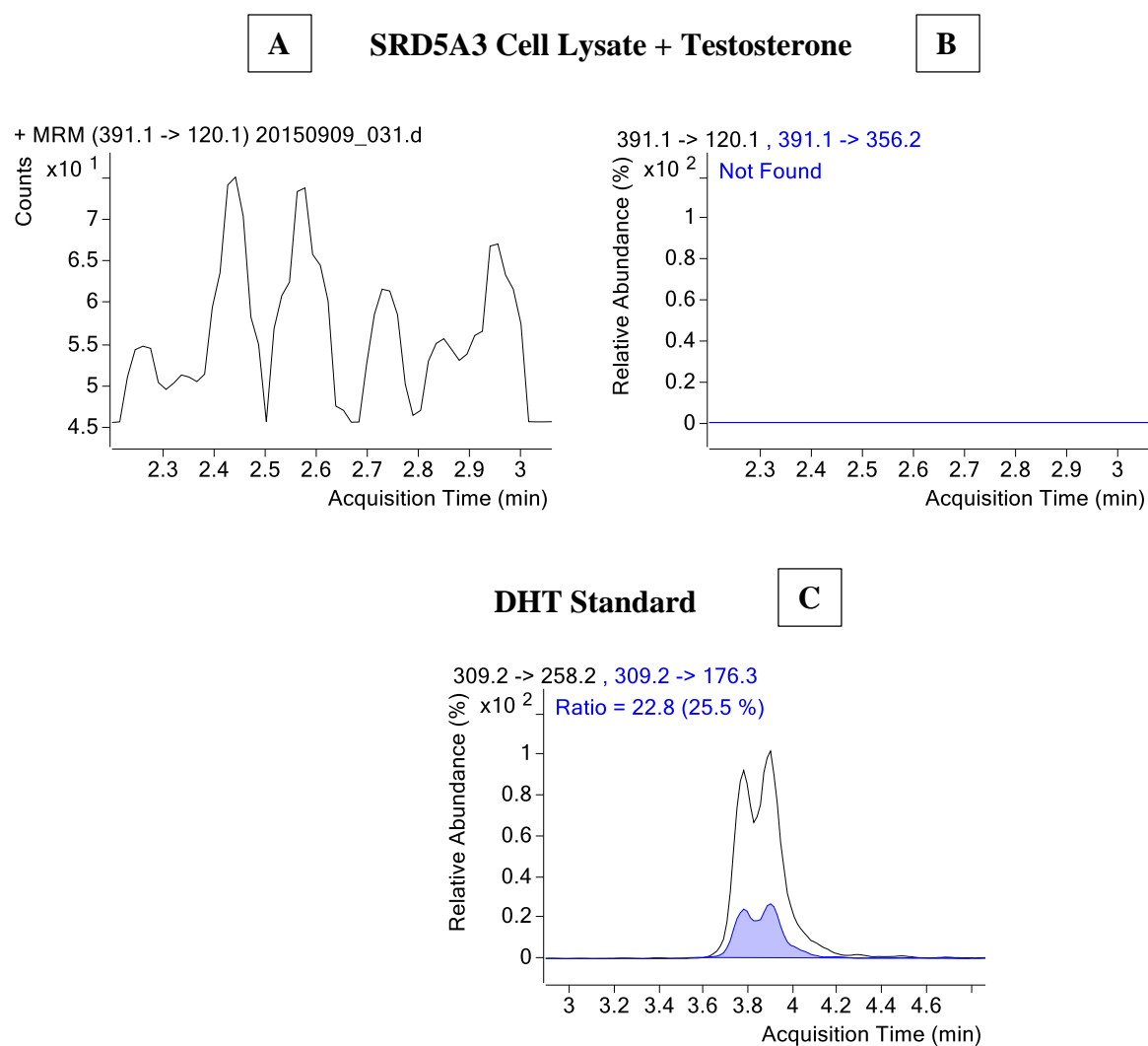


Figure 7. HEK293 cell lysate did reduce testosterone to DHT. The addition of testosterone to HEK293 cells did not result in the detection of DHT by mass spectrometry (Panels A, B). The DHT retention time, ratio of qualifier/quantifier ion, does not correspond to results obtained with the DHT internal standard (Panel C).

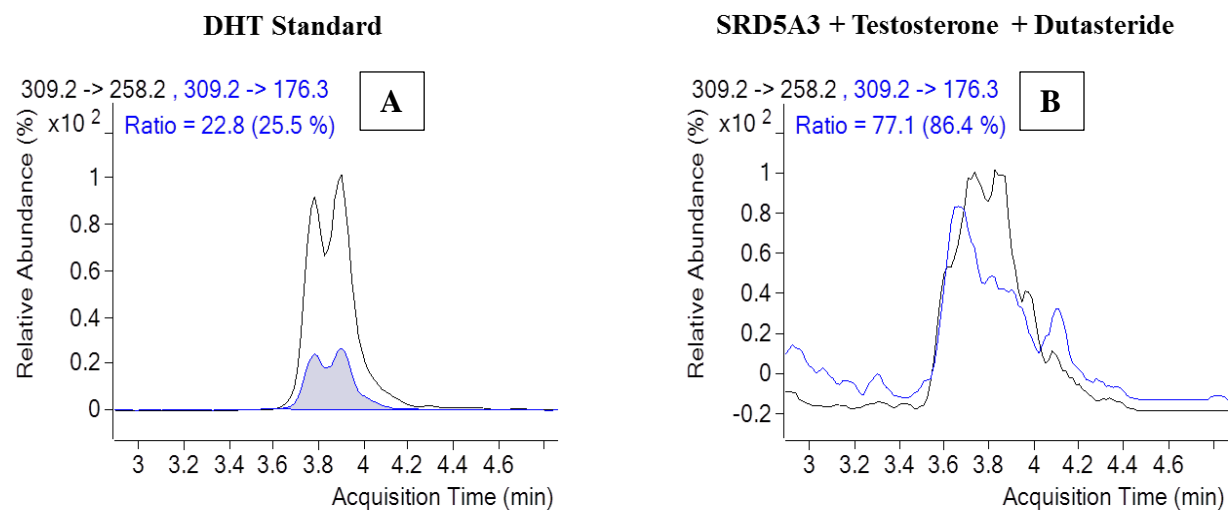
**Figure 8. Conversion of Testosterone to DHT with Addition of Dutasteride**

Figure 8. DHT internal standard showing a double peak at an elution time of 3.901 minutes (Panel A). No DHT peak was detected following the addition of 10 $\mu$ M testosterone with 1 nM dutasteride to HEK293 cells transfected with the *SRD5A3* expression vector.

**Figure 9. SRD5A3 Protein Inhibition by Dutasteride**

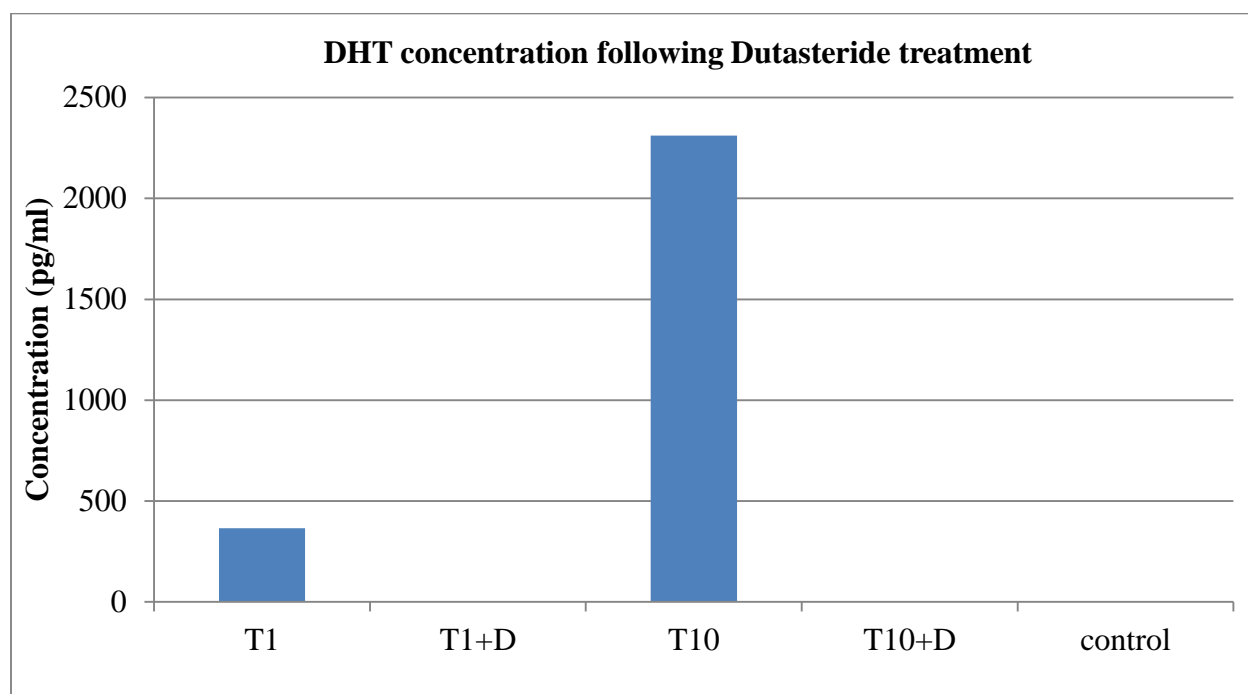


Figure 9. The addition of testosterone to HEK293 cells transfected with the *SRD5A3* vector resulted in the production of DHT. The addition of 10  $\mu$ M of testosterone (T10) resulted in a significantly higher amount of DHT detected compared to 1  $\mu$ M of testosterone (T1). The addition of dutasteride (D) to T1 and T10 inhibited the conversion of testosterone to DHT, and no DHT was detected or quantified. The control cells had no detectable DHT.

### 3.42. Progesterone

C-13 labeled progesterone at 1 and 10  $\mu\text{M}$  was added to HEK 293 transfected cells. The conversion of progesterone to its 5-alpha reduced product, dihydroprogesterone, was not detected at either concentration by mass spectrometry (Figure 10).

**Figure 10. Conversion of Progesterone to Dihydroprogesterone by SRD5A3**

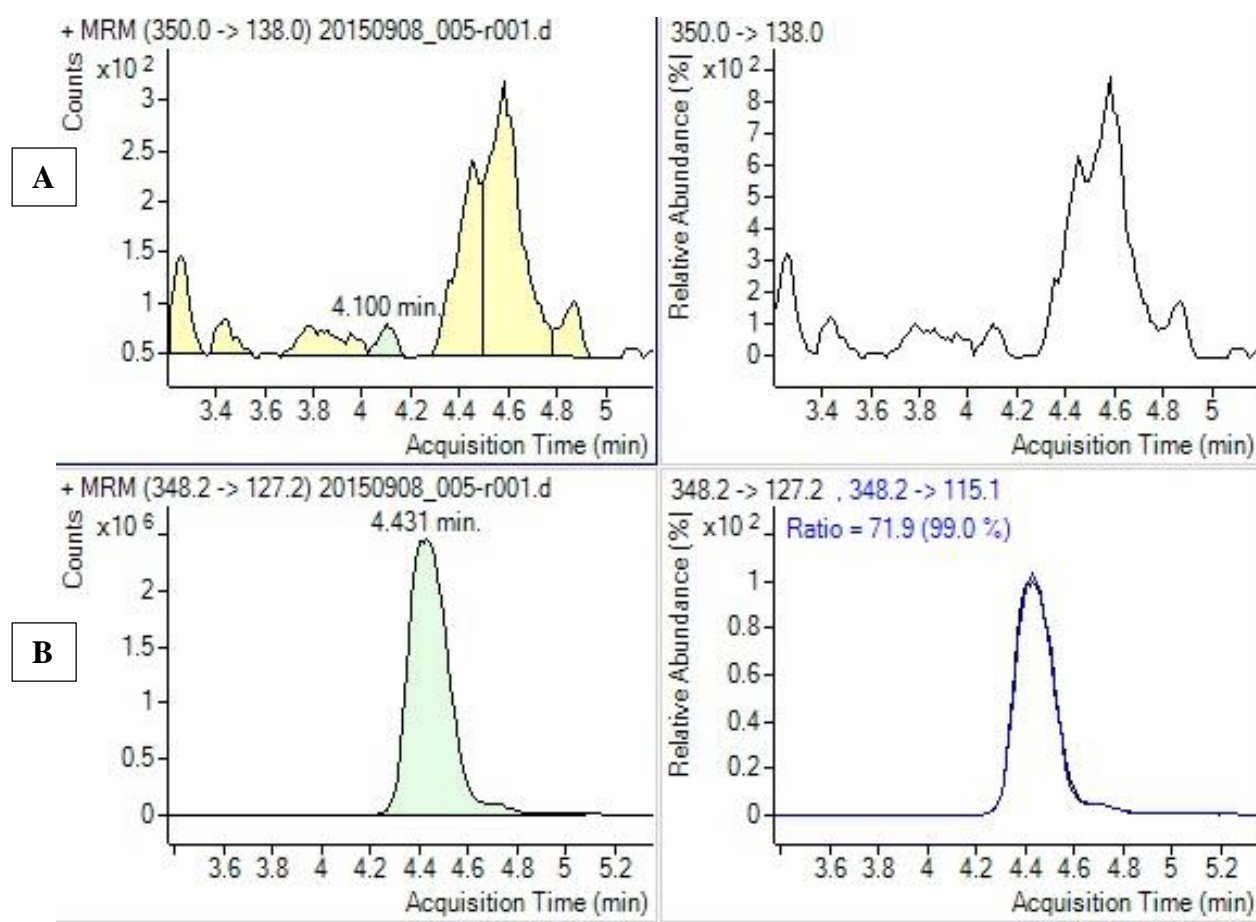


Figure 10. HEK293 cells transfected with SRD5A3 vector did not convert progesterone to the 5-alpha reduced product, dihydroprogesterone. The addition of progesterone to HEK293 cells did not result in the detection of dihydroprogesterone (Panel A). The internal standard for progesterone shows a peak eluting at 4.2-4.6 minutes (Panel B).

### 3.43. *Androstenedione*

C-13 labeled androstenedione at 1 and 10  $\mu$ M was added to HEK 293 transfected cells. Mass spectrometry analysis did not detect the conversion of androstenedione to its 5-alpha reduced product, androstanedione, at either concentration. (Figure 11).

**Figure 11. Conversion of Androstenedione to Androstanedione by SRD5A3**

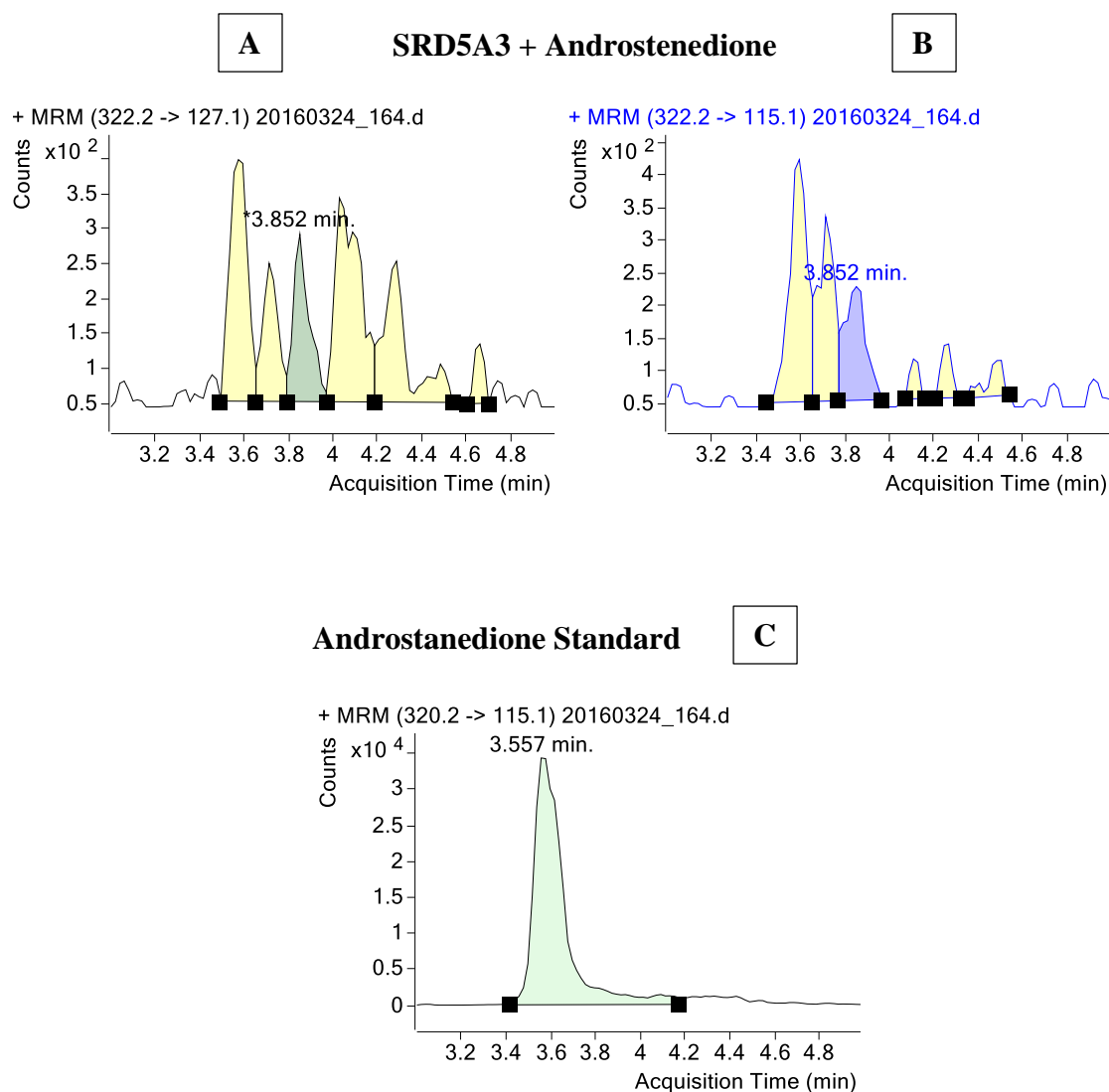


Figure 11. HEK293 cells transfected with SRD5A3 vector did not convert androstenedione to the 5- $\alpha$  reduced product, androstanedione. The androstanedione retention time (Panel A), qualifier and quantifier ratio (Panel B), does not correspond to the androstanedione standard (Panel C).

### 3.44. *Epitestosterone*

Epitestosterone at 1 and 10  $\mu\text{M}$  was added to HEK293 transfected cells. Mass spectrometry analysis revealed a peak associated with the formation of the 5-alpha reduced product of epitestosterone at both concentrations. This is based on the correct transition similar to testosterone, and correct retention time based on the testosterone to DHT standard available (Figure 12). The addition of 10  $\mu\text{M}$  epitestosterone resulted in a two-fold increase in the conversion to the reduced product compared to the addition of 1  $\mu\text{M}$  of epitestosterone. The addition of dutasteride significantly decreased the conversion of epitestosterone to its 5-alpha reduced product at both 1  $\mu\text{M}$  and 10  $\mu\text{M}$  concentrations ( $p < 0.05$ ) (Figure 13).

**Figure 12. 5-alpha Reduction of Epitestosterone by SRD5A3**

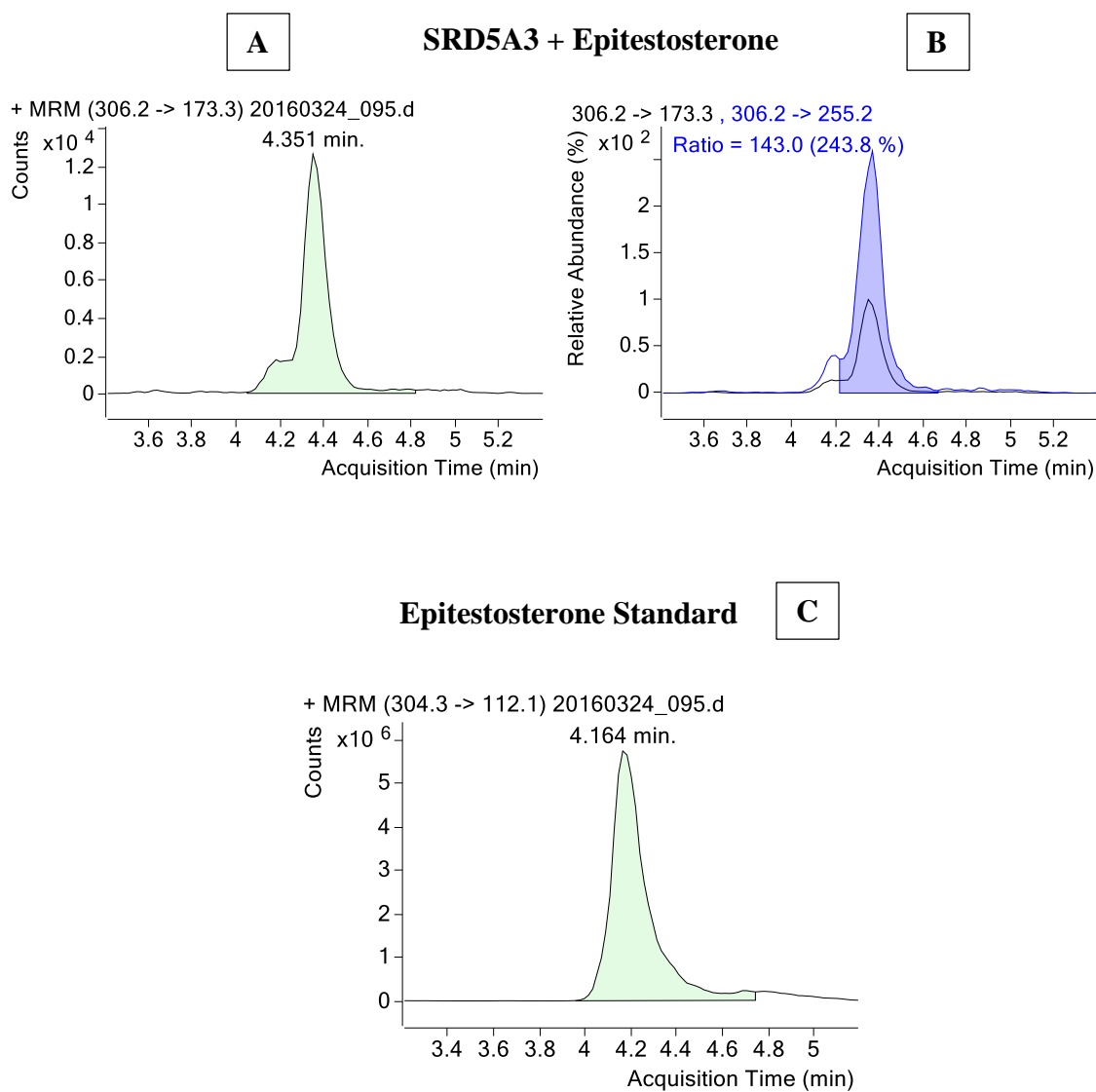


Figure 12. HEK293 cells transfected with SRD5A3 vector did convert epitestosterone to the 5-alpha reduced product. The resulting 5-alpha reduced product was detected and quantified using mass spectrometry. The peak eluting at 4.351 minutes (Panel A) was fragmented into a qualifier and quantifier ion (Panel B). The epitestosterone standard is shown in Panel C, with a peak eluting at 4.164 minutes.

**Figure 13. SRD5A3 Protein Inhibition by Dutasteride – Epitestosterone**

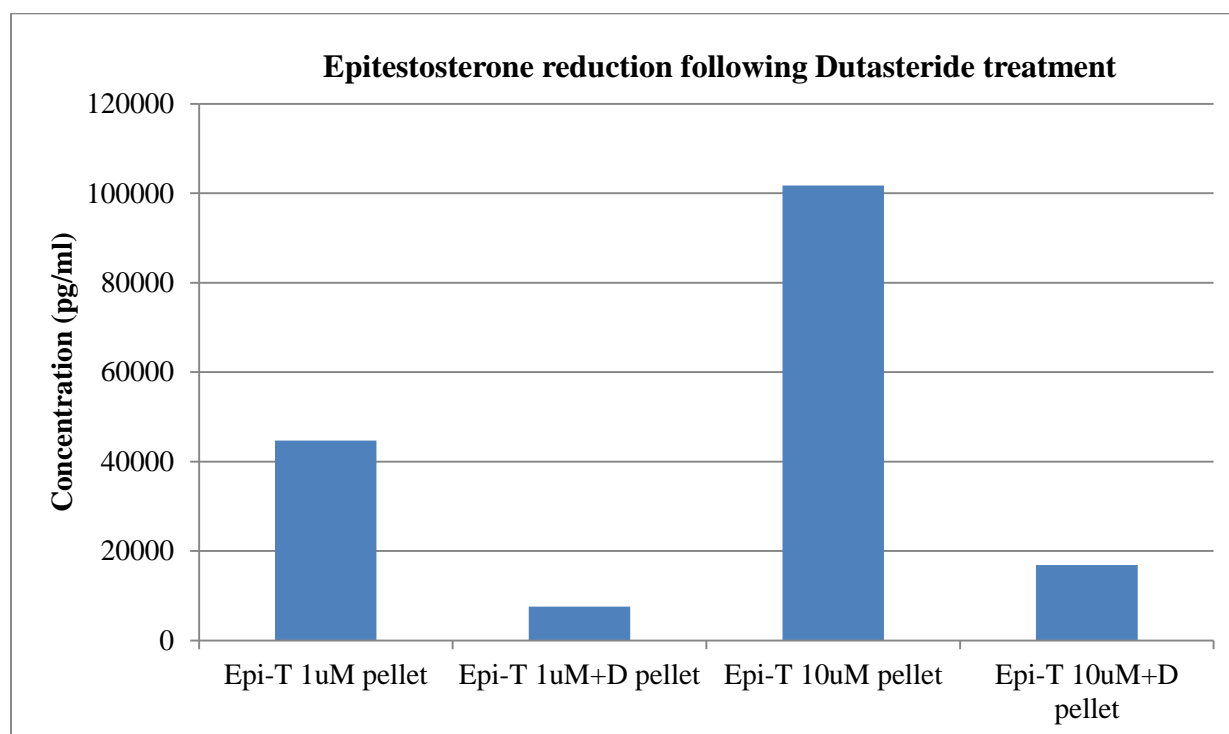


Figure 13. The addition of epitestosterone to HEK293 cells transfected with the *SRD5A3* vector resulted in the production of the corresponding 5-alpha reduced product. The addition of 10  $\mu$ M of epitestosterone resulted in a higher amount of product detected compared to 1  $\mu$ M of epitestosterone. The addition of dutasteride (D) to 1 and 10  $\mu$ M of epitestosterone resulted in a significant decrease in the conversion of epitestosterone to its 5-alpha reduced product.

### 3.45. 6- $\beta$ -hydroxytestosterone

6- $\beta$ -hydroxytestosterone at 1 and 10  $\mu$ M was added to HEK293 transfected cells. Mass spectrometry analysis revealed a peak associated with the formation of the 5- $\alpha$  reduced product of 6- $\beta$ -hydroxytestosterone (Figure 14). There was a two-fold increase in the amount 5- $\alpha$  reduced product formed between the 1  $\mu$ M and 10  $\mu$ M concentrations of 6- $\beta$ -hydroxytestosterone added. The addition of dutasteride significantly decreased the reduction of 6- $\beta$ -hydroxytestosterone at 1  $\mu$ M concentration ( $p < 0.05$ ), but not at 10  $\mu$ M concentration ( $p > 0.05$ ) (Figure 15).

**Figure 14. 5- $\alpha$  Reduction of 6- $\beta$ -hydroxytestosterone by SRD5A3**

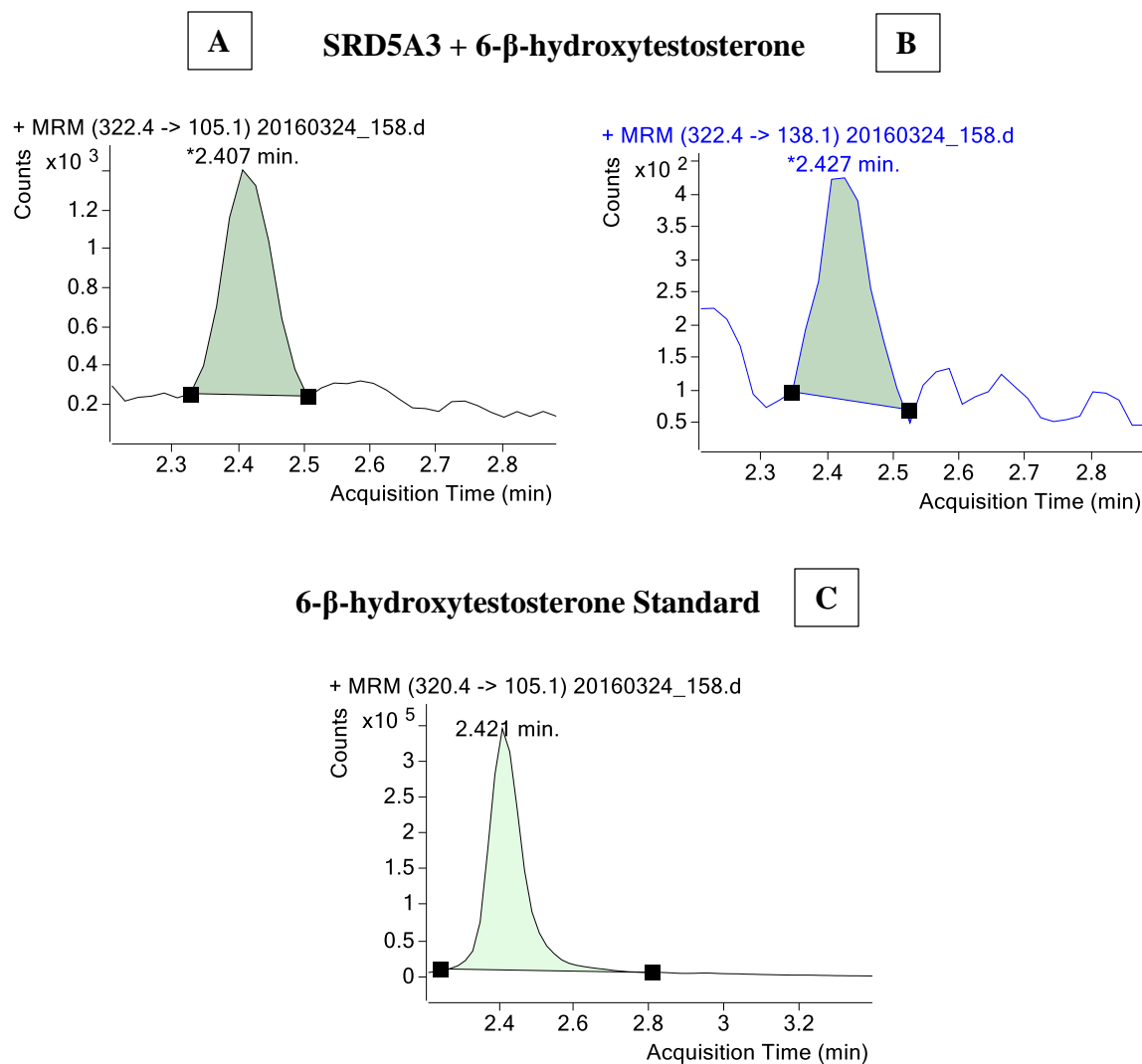


Figure 14. HEK293 cells transfected with SRD5A3 did convert 6- $\beta$ -hydroxytestosterone to the 5- $\alpha$  reduced product. The resulting 5- $\alpha$  reduced product was detected and quantified using mass spectrometry. The peak eluting at 2.407 minutes (Panel A) was fragmented into a qualifier and quantifier ion (Panel B). The 6- $\beta$ -hydroxytestosterone standard is shown in Panel C, with a peak eluting at 2.421 minutes.

**Figure 15. SRD5A3 Protein Inhibition by Dutasteride - 6- $\beta$ -hydroxytestosterone**

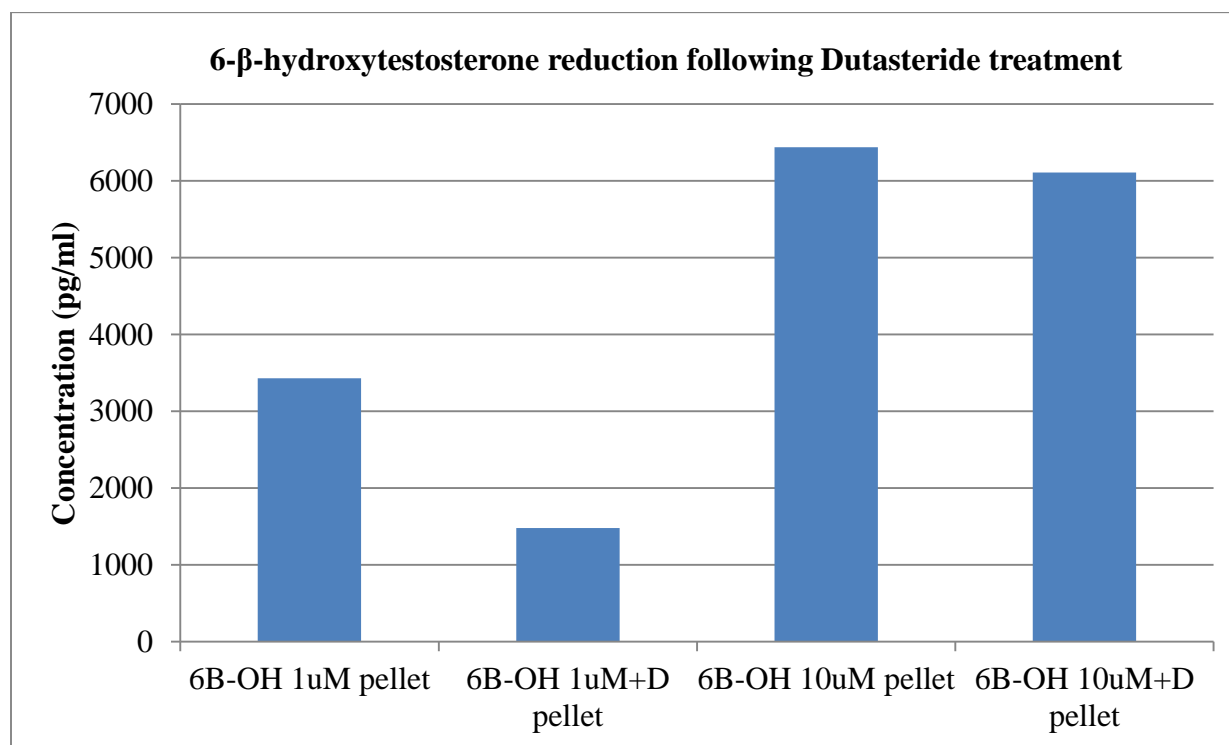


Figure 15. The addition of 6- $\beta$ -hydroxytestosterone to HEK293 cells transfected with the *SRD5A3* vector resulted in the production of the corresponding 5- $\alpha$  reduced product. The addition of 10  $\mu$ M of 6- $\beta$ -hydroxytestosterone resulted in a higher amount of product detected compared to 1  $\mu$ M of 6- $\beta$ -hydroxytestosterone. The addition of dutasteride (D) significantly decreased the reduction of 6- $\beta$ -hydroxytestosterone at 1  $\mu$ M, but not at 10  $\mu$ M.

### 3.46. 11- $\beta$ -hydroxytestosterone

11- $\beta$ -hydroxytestosterone at 1 and 10  $\mu$ M was added to HEK293 transfected cells. Mass spectrometry analysis revealed a peak associated with the formation of the 5- $\alpha$  reduced product of 11- $\beta$ -hydroxytestosterone (Figure 16). There is an almost three-fold increase in the amount of 5- $\alpha$  reduced product formed between the 1  $\mu$ M and 10  $\mu$ M concentrations of 11- $\beta$ -hydroxytestosterone. The addition of dutasteride (D) significantly decreased the reduction of 11- $\beta$ -hydroxytestosterone at 1  $\mu$ M concentration ( $p < 0.05$ ), but not at 10  $\mu$ M concentration ( $p > 0.05$ ) (Figure 17).

**Figure 16. 5- $\alpha$  Reduction of 11- $\beta$ -hydroxytestosterone by SRD5A3**

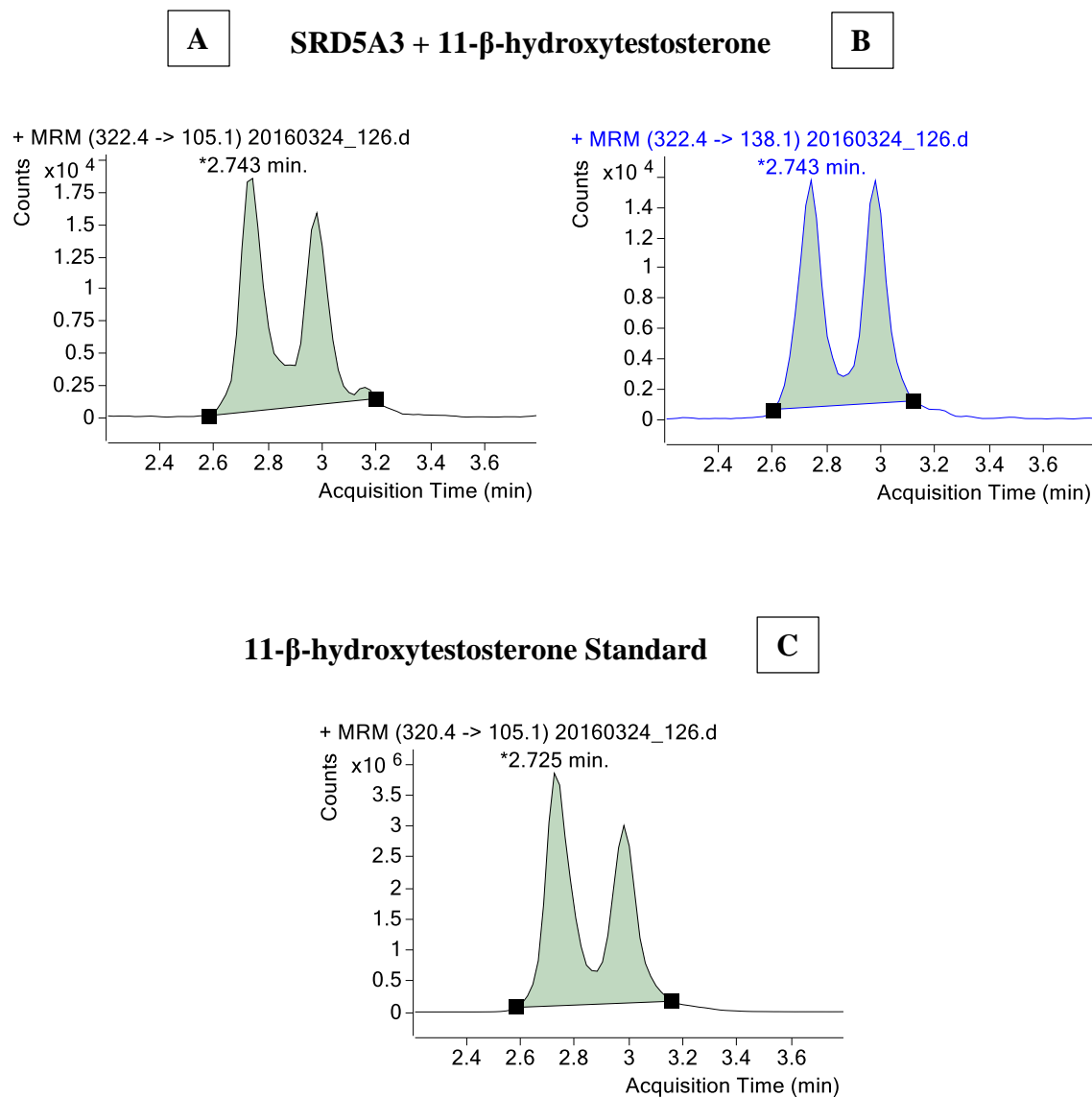


Figure 16. HEK293 cells transfected with SRD5A3 vector did convert 11- $\beta$ -hydroxytestosterone to the 5- $\alpha$  reduced product. The resulting 5- $\alpha$  reduced product was detected and quantified using mass spectrometry. The peak eluting at 2.743 minutes (Panel A) was fragmented into a qualifier and quantifier ion (Panel B). The 11- $\beta$ -hydroxytestosterone standard is shown in Panel C, with a peak eluting at 2.725 minutes.

**Figure 17. SRD5A3 Protein Inhibition by Dutasteride - 11- $\beta$ -hydroxytestosterone**

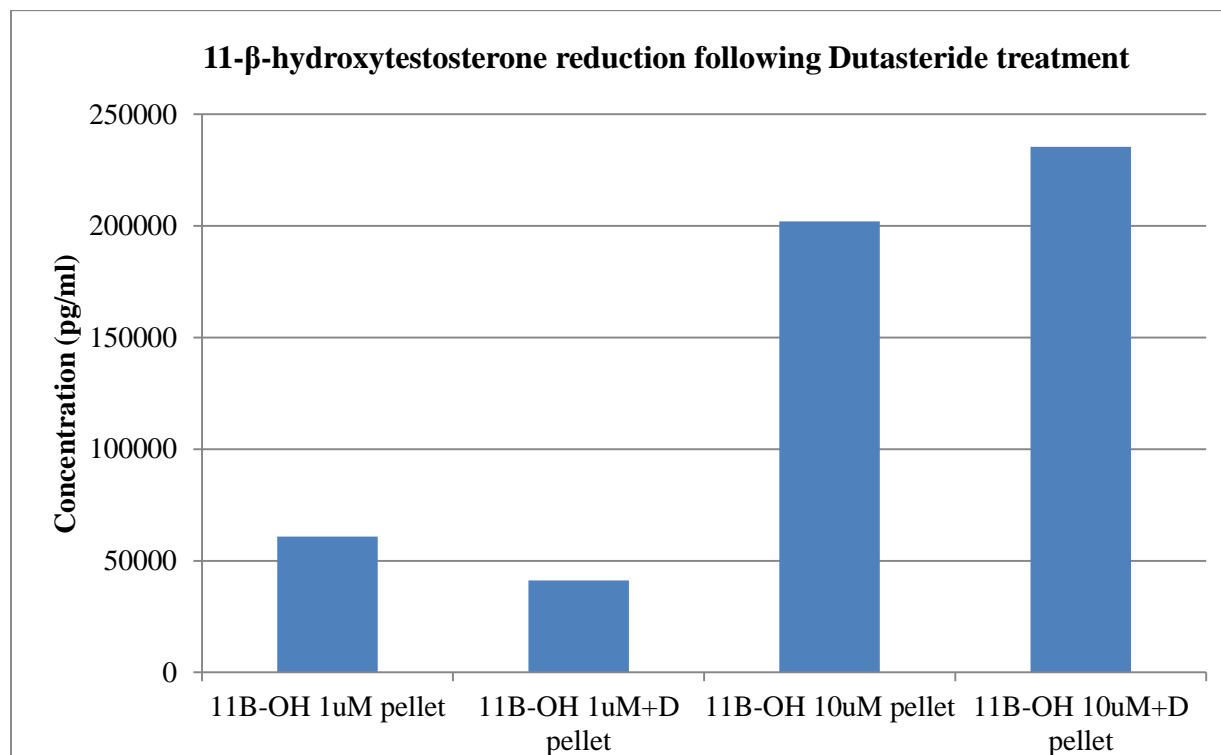


Figure 17. The addition of 11- $\beta$ -hydroxytestosterone to HEK293 cells transfected with the *SRD5A3* vector resulted in the production of the corresponding 5- $\alpha$  reduced product. The addition of 10  $\mu$ M of 11- $\beta$ -hydroxytestosterone resulted in a higher amount of product detected compared to 1  $\mu$ M of 11- $\beta$ -hydroxytestosterone. The addition of dutasteride (D) significantly decreased the reduction of 11- $\beta$ -hydroxytestosterone at 1  $\mu$ M, but not at 10  $\mu$ M.

### 3.47. *11- $\alpha$ -hydroxytestosterone*

11- $\alpha$ -hydroxytestosterone at 1 and 10  $\mu$ M was added to HEK293 transfected cells. Mass spectrometry analysis revealed a peak associated with the formation of the 5- $\alpha$  reduced product of 11- $\beta$ -hydroxytestosterone (Figure 18). The addition of 10  $\mu$ M of 11- $\alpha$ -hydroxytestosterone resulted in an increased quantity of reduced product formed. The addition of dutasteride did not decrease 5- $\alpha$  reduced product formation at either 1 or 10  $\mu$ M of 11- $\alpha$ -hydroxytestosterone.

**Figure 18. 5- $\alpha$  Reduction of 11- $\alpha$ -hydroxytestosterone by SRD5A3**

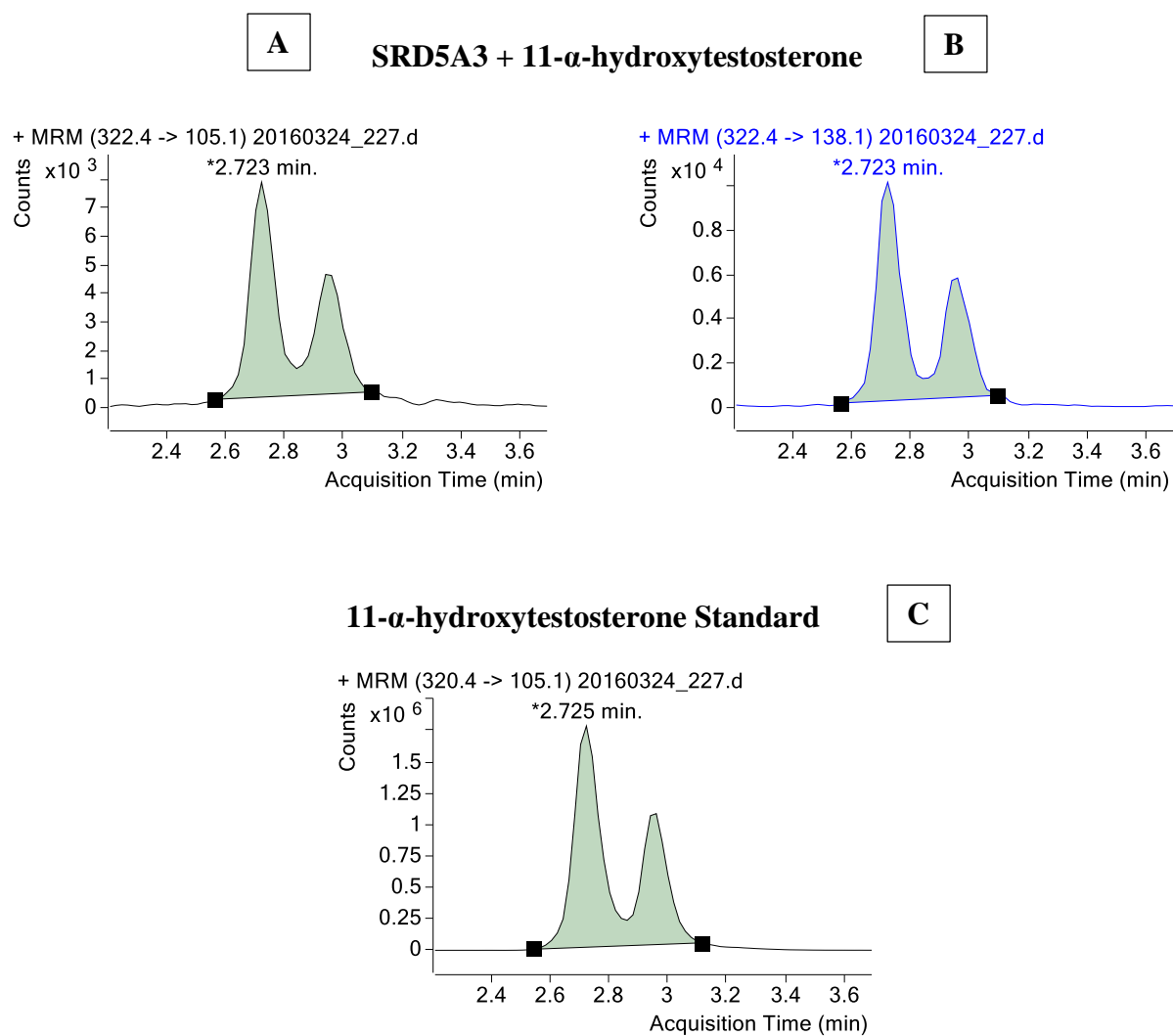


Figure 18. HEK293 cells transfected with SRD5A3 vector did convert 11- $\alpha$ -hydroxytestosterone to the 5- $\alpha$  reduced product. The resulting 5- $\alpha$  reduced product was detected and quantified using mass spectrometry. The peak eluting at 2.723 minutes (Panel A) was fragmented into a qualifier and quantifier ion (Panel B). The 11- $\alpha$ -hydroxytestosterone standard is shown in Panel C, with a peak eluting at 2.725 minutes.

**Figure 19. SRD5A3 Protein Inhibition by Dutasteride - 11- $\alpha$ -hydroxytestosterone**

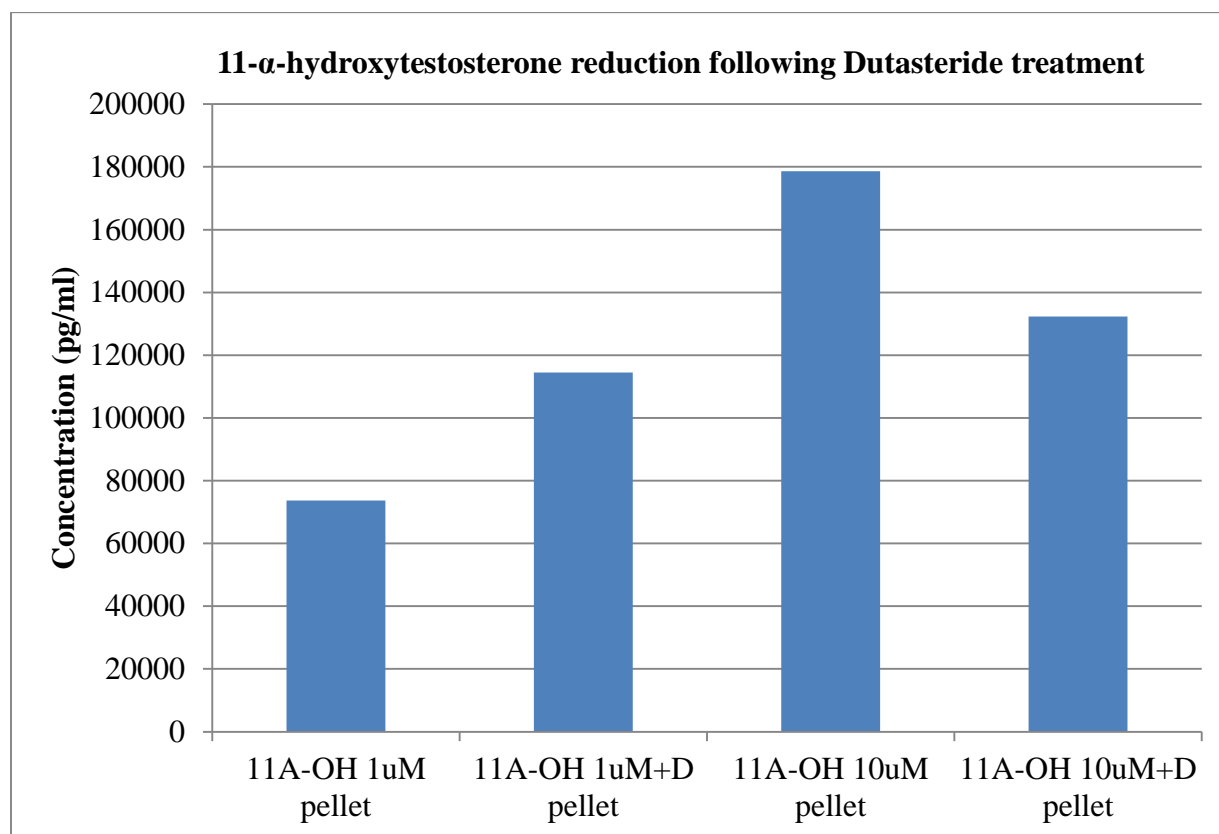


Figure 19. The addition of 11- $\alpha$ -hydroxytestosterone to HEK293 cells transfected with the *SRD5A3* vector resulted in the production of the corresponding 5- $\alpha$  reduced product. The addition of 10  $\mu$ M of 11- $\alpha$ -hydroxytestosterone resulted in a higher amount of product detected compared to 1  $\mu$ M of 11- $\alpha$ -hydroxytestosterone. The addition of dutasteride (D) did not consistently affect the conversion of 11- $\alpha$ -hydroxytestosterone to the 5- $\alpha$  reduced product.

### 3.48. *11-ketotestosterone*

11-ketotestosterone at 1 and 10  $\mu\text{M}$  was added to HEK293 transfected. Mass spectrometry analysis revealed a peak corresponding to 11-ketoDHT, the 5-alpha reduced product of 11-ketotestosterone (Figure 20). The addition of dutasteride to both the 1 and 10  $\mu\text{M}$  concentrations of 11-ketotestosterone did not result in a significant difference in the amount of 11-ketoDHT formed (Figure 21).

**Figure 20- 5-alpha Reduction of 11-ketotestosterone by SRD5A3**

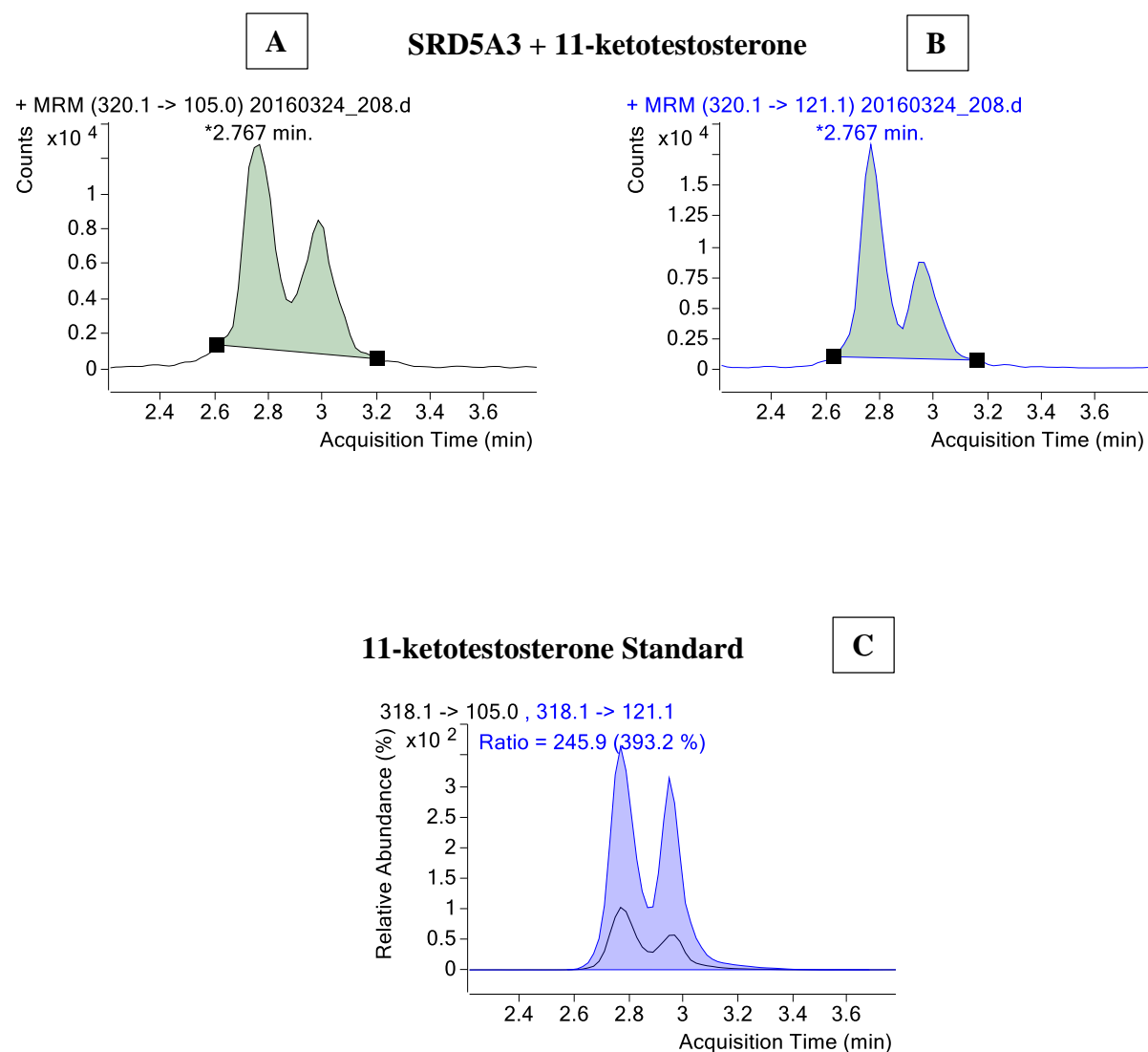


Figure 18. HEK293 cells transfected with SRD5A3 vector did convert 11-ketotestosterone to the 5-alpha reduced product, 11-ketoDHT. 11-ketoDHT was detected and quantified using mass spectrometry. The peak eluting at 2.767 minutes (Panel A) was fragmented into a qualifier and quantifier ion (Panel B). The 11-ketotestosterone standard is shown in Panel C.

**Figure 21. SRD5A3 Protein Inhibition by Dutasteride - 11-ketotestosterone**

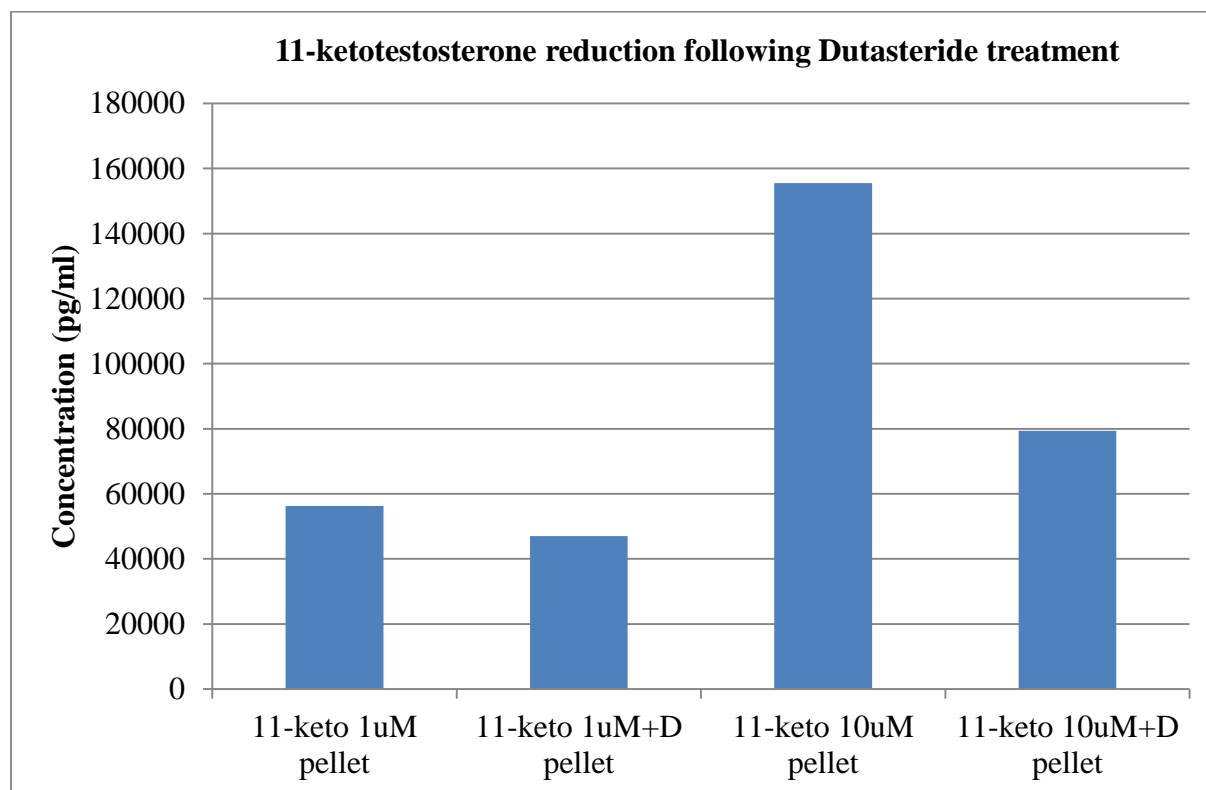


Figure 19. The addition of 11-ketotestosterone to HEK293 cells transfected with the *SRD5A3* vector resulted in the production of the corresponding 5-alpha reduced product, 11-ketoDHT. The addition of 10  $\mu$ M of 11-ketotestosterone resulted in a higher amount of product detected compared to 1  $\mu$ M of 11-ketotestosterone. The addition of dutasteride (D) did not significantly change the amount of 11-ketoDHT produced at 1  $\mu$ M, but did significantly decrease the conversion at 10  $\mu$ M of 11-ketotestosterone.

## **CHAPTER 4: DISCUSSION**

The 5-alpha reductase enzyme family plays an important role in the conversion of steroid precursors to their 5-alpha reduced products, such as the conversion of testosterone to the more potent androgen, DHT (16, 53). Androgen deprivation therapy aimed at reducing levels of circulating testosterone, and subsequently DHT, is well established as first line therapy for prostate cancer (54). 5-alpha reductase inhibitors, such as finasteride and dutasteride, have the capacity of inhibiting the conversion of testosterone to DHT (55). However, despite showing activity in reducing the incidence of prostate cancer development in preventive studies, the role of 5-alpha reductase inhibitors in prostate cancer prevention remains controversial (3, 9, 13). In addition, 5-alpha reductase inhibitors are not currently included in the treatment guidelines for prostate cancer, as they have not shown convincing clinical activity in this setting (2). The distribution and function of 5-alpha reductase 1 and 2 have been well characterized in the normal prostate as well as prostate cancer (4). This study aimed at shedding light on the enzymatic activity of a newer member of the 5-alpha reductase family of enzymes, SRD5A3, in steroidogenesis and prostate carcinogenesis.

SRD5A3 cDNA ORF was transfected into HEK293 cells using the OriGene vector system. This is different from the HP-Thioredoxin-fusion SRD5A3 protein using a pBAD/Thio-TOPO vector used by Titus et al. (51), and the FuGENE 6 vector used by Uemura et al.(5). Using this vector, the SRD5A3 plasmid was successfully transfected into HEK293 cells. Transient and stable transfections were verified by immunoblot assays using an anti-DDK antibody revealing a band at 37 kDa, corresponding to the SRD5A3 protein (Figure 3). Conversely, the anti-SRD5A3 antibody did not yield a positive immunoblot result, despite the addition of increasing concentrations of SRD5A3 into the immunoblot wells. These results

suggest that the anti-DDK antibody may be a more sensitive tool to detect successfully SRD5A3 transfection using the OriGene vector with an anti-DDK tag.

Mass spectrometry analysis revealed that HEK293 transfected cells did convert C-13 labeled testosterone to DHT (Figure 5). This activity was concentration dependent, with higher levels of testosterone yielding a higher DHT levels (Figure 9). This report confirms prior observations by Uemura et al. using a different transfection system (5), and Titus et al. using a fusion SRD5A3 protein (51). The conversion of C-13 labeled testosterone to DHT was only observed in intact HEK293 transfected cells. Mass spectrometry analysis of a cell lysate of HEK293 transfected cells did not detect any DHT production following the addition of C-13 labeled testosterone (Figure 7). This is in contrast to the study by Titus et al. where HP-Thioredoxin-fusion SRD5A3 protein using a pBAD/Thio-TOPO vector showed 5-alpha reducing activity in both intact cells and cell lysate (51). Conversely, another study evaluated hamster SRD5A3 expressed as a fusion protein with green fluorescent protein from the pcDNA3.1-NT-GFP/hSrd5a3 plasmid and human SRD5A3. In that study, the fusion protein localized to the cytoplasm and did not show steroid reducing capacity (52). These findings in addition to the known role of SRD5A3 role in N-linked glycosylation of surface proteins (45), suggest that SRD5A3 exerts its 5-alpha reducing activity mainly when intact in the plasma membrane.

This study also aimed at evaluating the ability of SRD5A3 to reduce testosterone analogues. The development of castrate resistant prostate cancer despite low testosterone levels has generated interest in looking for other steroid substrates able to active the androgen receptor under castrate conditions. Castrate resistant prostate cancer appears to possess the machinery to bypass testosterone and use adrenal androgens, such as dehydroepiandrosterone and androstenedione, to produce intratumoral DHT through a “backdoor steroid pathway” (16, 20,

56). Additionally, more recent studies have expanded the list of adrenal androgens that may potentially be involved in the development of castrate resistant prostate cancer (31, 57). 11-hydroxyandrostenedione is an abundant adrenal androgen which has limited ability to activate the androgen receptor. Through the action of 17 $\beta$ -hydroxysteroid dehydrogenase and 11 $\beta$ -hydroxysteroid dehydrogenase enzymes, 11-hydroxyandrostenedione is converted to 11-ketotestosterone. Subsequently, 11-ketotestosterone is 5-alpha reduced to 11-ketoDHT, a steroid as potent as DHT in its ability to active the androgen receptor (31, 57). These studies have shed light on the role of 5-alpha reductases 1 and 2 in this “backdoor steroid pathway”. However, the role of SRD5A3 in this setting has not been studied yet. In our study, the addition of testosterone analogues (epitestosterone, 11-hydroxytestosterone, 6- $\beta$ -hydroxytestosterone, 11- $\beta$ -hydroxytestosterone, 11- $\alpha$ -hydroxytestosterone, and 11-ketotestosterone) resulted in the production of the respective 5-alpha reduced counterparts. These findings, in addition to SRD5A3 being almost ubiquitous in the body (49, 50), suggests that this enzyme may be involved in the conversion of circulating steroid precursors to more potent androgens capable of activating the androgen receptor. Developing a model containing SRD5A3, the androgen receptor gene, as well as linked reporter assay such as luciferase would demonstrate activation of the androgen receptor. In addition, such a reporter assay can potentially allow quantification of the androgen receptor activation depending on the precursor steroid added to the system.

Additionally, SRD5A3 is upregulated under androgen deprivation therapy (32), potentially magnifying its role in the reduction of circulating androgens capable of binding the androgen receptor to activate gene targets and downstream signaling. This potentially implicates SRD5A3 in the non-canonical steroid pathway which is hypothesized to drive castrate resistant prostate cancer even in the presence of castrate levels of testosterone. Mass spectrometry

analysis can be performed to compare the levels of circulating adrenal androgens between castrate-sensitive and castrate-resistant prostate cancer samples, in the setting of castrate levels of testosterone. Circulating adrenal androgens levels, along with their respective potencies in activating the androgen receptor, can be helpful in determining their role in driving androgen receptor signaling.

These findings, along with previous studies linking adrenal androgens to the production of potent androgen receptor ligands suggest that measuring peripheral blood testosterone levels alone may not fully reflect the circulating steroid burden that can potentially drive prostate cancer growth. A more accurate assessment of castrate androgen levels may be obtained by evaluating a panel of circulating androgens shown to bind and androgen receptor signaling.

Furthermore, this study aimed to evaluate the effect of dutasteride, a known 5- $\alpha$  reductase 1 and 2 inhibitor, on the enzymatic activity of SRD5A3. Titus et al. previously reported that dutasteride partially inhibited the conversion of testosterone to DHT in a HP-Thioredoxin-fusion SRD5A3 enzyme system (51). Using an SRD5A3 cDNA ORF transfected into HEK293 cells using the OriGene vector system, our findings suggest that the inhibitory effect of dutasteride on SRD5A3 is substrate dependent. Dutasteride completely inhibited the conversion of testosterone to DHT at both 1 and 10  $\mu$ M concentrations of testosterone. When added to epitestosterone, dutasteride significantly decreased but did not completely eliminate the conversion of epitestosterone to the 5- $\alpha$  reduced product at both the 1 and 10  $\mu$ M concentrations. For 6- $\beta$ -hydroxytestosterone and 11- $\beta$ -hydroxytestosterone, dutasteride significantly decreased the conversion to their respective 5- $\alpha$  reduced products at 1  $\mu$ M, but not at the 10  $\mu$ M concentration. Finally, dutasteride did not inhibit the conversion of 11- $\alpha$ -hydroxytestosterone or 11-ketotestosterone at either the 1 or 10  $\mu$ M concentrations.

These results suggest that the interaction between the steroid substrate and the SRD5A3 enzyme affects the inhibitory activity of dutasteride. The androgen substrate conformation and location of hydroxyl and ketone groups may dictate the potential for drugs such as dutasteride to bind SRD5A3 and inhibit its catalytic 5- $\alpha$  reducing function. Similarly to previously described activity with 5- $\alpha$  reductases 1 and 2 (55), dutasteride inhibited the conversion of testosterone to DHT by SRD5A3. Interestingly, dutasteride reduced but did not fully eliminate the conversion of epitestosterone, an epimer of testosterone, to its 5- $\alpha$  reduced product. Furthermore, with variations in the location of hydroxyl and ketone groups in testosterone analogues, the inhibitory potential of dutasteride on SRD5A3 appeared to be weaker. A higher concentration (10  $\mu$ M) of 6- $\beta$ -hydroxytestosterone and 11- $\beta$ -hydroxytestosterone was able to overcome the inhibitory activity of dutasteride on SRD5A3. This suggests that the mechanism of action of dutasteride with these specific substrates may be through competitive inhibition. Finally, dutasteride had no effect on the 5- $\alpha$  reducing capacity of SRD5A3 when 11- $\alpha$ -hydroxytestosterone or 11-ketotestosterone were added to HEK293 transfected cells.

These findings suggest that further investigation is warranted to understand the structure activity relationship of the SRD5A3-dutasteride enzyme-substrate complex. This knowledge may shed light on the reasons underlying the variation in dutasteride inhibitory activity on SRD5A3 based on the type and polarity of androgen substrates. Additionally, given the differences in properties between various 5- $\alpha$  reductase enzymes, and between 5- $\alpha$  reductase inhibitors, it is imperative to determine if dutasteride is the optimal 5- $\alpha$  reductase inhibitor to target SRD5A3.

The mass spectrometry findings suggest that SRD5A3 has the capacity of reducing steroid substrates into potent androgens that have been shown to activate the androgen receptor

(31, 57). In this closed system, dutasteride lacks the capacity to inhibit SRD5A3 5-alpha reducing capacity across all androgen substrates. In vivo studies measuring circulating adrenal androgens prone to becoming 5-alpha reductase substrates are mandated to evaluate the overall androgen burden that may be contributing to prostate carcinogenesis. Findings from such studies, in conjunction with ubiquitous distribution of SRD5A3 in the body (49, 50), can potentially magnify this enzyme's role in the development of castrate resistant prostate cancer. This would provide a basis for the discovery of targeted SRD5A3 inhibiting drugs, to be used in rational therapeutic combinations across the spectrum of prostate cancer. This would include, but not limited to prostate cancer prevention, preoperative therapy for prostate cancer, and the prevention and treatment of castrate resistant prostate cancer.

## **CHAPTER 5: CONCLUSION**

In conclusion, this study confirmed that, within an in-vitro system, SRD5A3 has the capacity to convert testosterone and its derivatives to their more potent, 5-alpha reduced, products, capable of binding and activating androgen receptor signaling. The inhibitory activity of dutasteride, a known 5-alpha reductase 1 and 2 inhibitor, on this enzyme, appears to be substrate and concentration dependent. These findings suggest a role for SRD5A3 in androgen metabolism and the development of the lethal phenotype of castrate resistant prostate cancer. In-vitro assessment of SRD5A3 is mandated to determine the potential role of therapeutic SRD5A3 inhibition across the spectrum of prostate cancer.

## **CHAPTER 6: LIMITATIONS**

There are several limitations to this study. First, SRD5A3 was evaluated in a closed in-vitro system. This likely doesn't replicate the intricate steroidogenic pathways and regulatory mechanisms in the human body, and less so in the presence of prostate cancer. Additionally, each steroid substrate was added separately into the system. This approach does not allow for the assessment of relative substrate affinity to SRD5A3. Furthermore, mass spectrometry internal standards for the 5-alpha reduced products of certain testosterone derivatives are not commercially available. Mass spectrometry analysis was carried out using standards extrapolated from the substrate compounds, or from previously published work in the literature (57). Finally, liquid chromatography-mass spectrometry is a highly sensitive tool that can detect compounds at minute quantities. This sensitive approach may lead to the detection of background noise which may contaminate the results, and lead to false positive conclusions.

## **CHAPTER 7: BIBLIOGRAPHY**

1. Hsing AW, Reichardt JK, Stanczyk FZ. Hormones and prostate cancer: current perspectives and future directions. *The Prostate*. 2002 Aug 1;52(3):213-35. PubMed PMID: 12111697.
2. Azzouni F, Mohler J. Role of 5alpha-reductase inhibitors in prostate cancer prevention and treatment. *Urology*. 2012 Jun;79(6):1197-205. PubMed PMID: 22446342.
3. Thompson IM, Goodman PJ, Tangen CM, Lucia MS, Miller GJ, Ford LG, Lieber MM, Cespedes RD, Atkins JN, Lippman SM, Carlin SM, Ryan A, Szczepanek CM, Crowley JJ, Coltman CA, Jr. The influence of finasteride on the development of prostate cancer. *The New England journal of medicine*. 2003 Jul 17;349(3):215-24. PubMed PMID: 12824459.
4. Titus MA, Gregory CW, Ford OH, 3rd, Schell MJ, Maygarden SJ, Mohler JL. Steroid 5alpha-reductase isozymes I and II in recurrent prostate cancer. *Clinical cancer research : an official journal of the American Association for Cancer Research*. 2005 Jun 15;11(12):4365-71. PubMed PMID: 15958619.
5. Uemura M, Tamura K, Chung S, Honma S, Okuyama A, Nakamura Y, Nakagawa H. Novel 5 alpha-steroid reductase (SRD5A3, type-3) is overexpressed in hormone-refractory prostate cancer. *Cancer science*. 2008 Jan;99(1):81-6. PubMed PMID: 17986282.
6. Sharifi N. Minireview: Androgen metabolism in castration-resistant prostate cancer. *Molecular endocrinology*. 2013 May;27(5):708-14. PubMed PMID: 23592429. Pubmed Central PMCID: 3634114.
7. Lebdaï S, Bigot P, Azzouzi AR. High-grade prostate cancer and finasteride. *BJU international*. 2010 Feb;105(4):456-9. PubMed PMID: 19930174.
8. Thomas LN, Lazier CB, Gupta R, Norman RW, Troyer DA, O'Brien SP, Rittmaster RS. Differential alterations in 5alpha-reductase type 1 and type 2 levels during development and

progression of prostate cancer. *The Prostate*. 2005 May 15;63(3):231-9. PubMed PMID: 15538746.

9. Andriole GL, Bostwick DG, Brawley OW, Gomella LG, Marberger M, Montorsi F, Pettaway CA, Tammela TL, Teloken C, Tindall DJ, Somerville MC, Wilson TH, Fowler IL, Rittmaster RS, Group RS. Effect of dutasteride on the risk of prostate cancer. *The New England journal of medicine*. 2010 Apr 1;362(13):1192-202. PubMed PMID: 20357281.

10. Roehrborn CG, Andriole GL, Wilson TH, Castro R, Rittmaster RS. Effect of dutasteride on prostate biopsy rates and the diagnosis of prostate cancer in men with lower urinary tract symptoms and enlarged prostates in the Combination of Avodart and Tamsulosin trial. *European urology*. 2011 Feb;59(2):244-9. PubMed PMID: 21093145.

11. Fleshner NE, Lucia MS, Egerdie B, Aaron L, Eure G, Nandy I, Black L, Rittmaster RS. Dutasteride in localised prostate cancer management: the REDEEM randomised, double-blind, placebo-controlled trial. *Lancet*. 2012 Mar 24;379(9821):1103-11. PubMed PMID: 22277570.

12. Kumar VL, Wahane VD. Current status of 5alpha-reductase inhibitors in the treatment of benign hyperplasia of prostate. *Indian journal of medical sciences*. 2008 Apr;62(4):167-75. PubMed PMID: 18445985.

13. Lacy JM, Kyprianou N. A tale of two trials: The impact of 5alpha-reductase inhibition on prostate cancer (Review). *Oncology letters*. 2014 Oct;8(4):1391-6. PubMed PMID: 25202340. Pubmed Central PMCID: 4156162.

14. Nacusi LP, Tindall DJ. Targeting 5alpha-reductase for prostate cancer prevention and treatment. *Nature reviews Urology*. 2011 Jul;8(7):378-84. PubMed PMID: 21629218. Pubmed Central PMCID: 3905570.

15. Shafi AA, Yen AE, Weigel NL. Androgen receptors in hormone-dependent and castration-resistant prostate cancer. *Pharmacology & therapeutics*. 2013 Dec;140(3):223-38. PubMed PMID: 23859952.
16. Luu-The V, Belanger A, Labrie F. Androgen biosynthetic pathways in the human prostate. *Best practice & research Clinical endocrinology & metabolism*. 2008 Apr;22(2):207-21. PubMed PMID: 18471780.
17. Dehm SM, Tindall DJ. Molecular regulation of androgen action in prostate cancer. *Journal of cellular biochemistry*. 2006 Oct 1;99(2):333-44. PubMed PMID: 16518832.
18. Debes JD, Tindall DJ. Mechanisms of androgen-refractory prostate cancer. *The New England journal of medicine*. 2004 Oct 7;351(15):1488-90. PubMed PMID: 15470210.
19. Gao J, Arnold JT, Isaacs JT. Conversion from a paracrine to an autocrine mechanism of androgen-stimulated growth during malignant transformation of prostatic epithelial cells. *Cancer research*. 2001 Jul 1;61(13):5038-44. PubMed PMID: 11431338.
20. Stanbrough M, Bubley GJ, Ross K, Golub TR, Rubin MA, Penning TM, Febbo PG, Balk SP. Increased expression of genes converting adrenal androgens to testosterone in androgen-independent prostate cancer. *Cancer research*. 2006 Mar 1;66(5):2815-25. PubMed PMID: 16510604.
21. Kumagai J, Hofland J, Erkens-Schulze S, Dits NF, Steenbergen J, Jenster G, Homma Y, de Jong FH, van Weerden WM. Intratumoral conversion of adrenal androgen precursors drives androgen receptor-activated cell growth in prostate cancer more potently than de novo steroidogenesis. *The Prostate*. 2013 Nov;73(15):1636-50. PubMed PMID: 23996639.
22. Locke JA, Guns ES, Lubik AA, Adomat HH, Hendy SC, Wood CA, Ettinger SL, Gleave ME, Nelson CC. Androgen levels increase by intratumoral de novo steroidogenesis during

progression of castration-resistant prostate cancer. *Cancer research*. 2008 Aug 1;68(15):6407-15.

PubMed PMID: 18676866.

23. Nakamura Y, Suzuki T, Nakabayashi M, Endoh M, Sakamoto K, Mikami Y, Moriya T, Ito A, Takahashi S, Yamada S, Arai Y, Sasano H. In situ androgen producing enzymes in human prostate cancer. *Endocr-Relat Cancer*. 2005 Mar;12(1):101-7. PubMed PMID:

WOS:000228049800007. English.

24. Mohler JL, Gregory CW, Ford OH, 3rd, Kim D, Weaver CM, Petrusz P, Wilson EM, French FS. The androgen axis in recurrent prostate cancer. *Clinical cancer research : an official journal of the American Association for Cancer Research*. 2004 Jan 15;10(2):440-8. PubMed PMID: 14760063.

25. Titus MA, Schell MJ, Lih FB, Tomer KB, Mohler JL. Testosterone and dihydrotestosterone tissue levels in recurrent prostate cancer. *Clinical cancer research : an official journal of the American Association for Cancer Research*. 2005 Jul 1;11(13):4653-7. PubMed PMID: 16000557.

26. Belanger B, Belanger A, Labrie F, Dupont A, Cusan L, Monfette G. Comparison of residual C-19 steroids in plasma and prostatic tissue of human, rat and guinea pig after castration: unique importance of extratesticular androgens in men. *Journal of steroid biochemistry*. 1989 May;32(5):695-8. PubMed PMID: 2525654.

27. Mizokami A, Koh E, Fujita H, Maeda Y, Egawa M, Koshida K, Honma S, Keller ET, Namiki M. The adrenal androgen Androstenediol is present in prostate cancer tissue after androgen deprivation therapy and activates mutated androgen receptor. *Cancer research*. 2004 Jan 15;64(2):765-71. PubMed PMID: WOS:000188399300045. English.

28. Nishiyama T, Hashimoto Y, Takahashi K. The influence of androgen deprivation therapy on dihydrotestosterone levels in the prostatic tissue of patients with prostate cancer. *Clinical cancer research : an official journal of the American Association for Cancer Research*. 2004 Nov 1;10(21):7121-6. PubMed PMID: 15534082.
29. Mitamura K, Nakagawa T, Shimada K, Namiki M, Koh E, Mizokami A, Honma S. Identification of dehydroepiandrosterone metabolites formed from human prostate homogenate using liquid chromatography-mass spectrometry and gas chromatography-mass spectrometry. *J Chromatogr A*. 2002 Jun 28;961(1):97-105. PubMed PMID: WOS:000177061200012. English.
30. Pelletier G. Expression of steroidogenic enzymes and sex-steroid receptors in human prostate. *Best Pract Res Cl En*. 2008 Apr;22(2):223-8. PubMed PMID: WOS:000256320400003. English.
31. Mostaghel EA. Beyond T and DHT - novel steroid derivatives capable of wild type androgen receptor activation. *International journal of biological sciences*. 2014;10(6):602-13. PubMed PMID: 24948873. Pubmed Central PMCID: 4062953.
32. Li J, Ding Z, Wang Z, Lu JF, Maity SN, Navone NM, Logothetis CJ, Mills GB, Kim J. Androgen regulation of 5alpha-reductase isoenzymes in prostate cancer: implications for prostate cancer prevention. *PloS one*. 2011;6(12):e28840. PubMed PMID: 22194926. Pubmed Central PMCID: 3237548.
33. Andriole GL, Humphrey P, Ray P, Gleave ME, Trachtenberg J, Thomas LN, Lazier CB, Rittmaster RS. Effect of the dual 5alpha-reductase inhibitor dutasteride on markers of tumor regression in prostate cancer. *The Journal of urology*. 2004 Sep;172(3):915-9. PubMed PMID: 15310997.

34. Iczkowski KA, Qiu J, Qian J, Somerville MC, Rittmaster RS, Andriole GL, Bostwick DG. The dual 5-alpha-reductase inhibitor dutasteride induces atrophic changes and decreases relative cancer volume in human prostate. *Urology*. 2005 Jan;65(1):76-82. PubMed PMID: 15667867.
35. Perrotti M, Jain R, Abriel LM, Baroni TE, Corbett AB, Tenenbaum SA. Dutasteride monotherapy in men with serologic relapse following radical therapy for adenocarcinoma of the prostate: a pilot study. *Urologic oncology*. 2012 Mar-Apr;30(2):133-8. PubMed PMID: 20800512.
36. Banez LL, Blake GW, McLeod DG, Crawford ED, Moul JW. Combined low-dose flutamide plus finasteride vs low-dose flutamide monotherapy for recurrent prostate cancer: a comparative analysis of two phase II trials with a long-term follow-up. *BJU international*. 2009 Aug;104(3):310-4. PubMed PMID: 19239458.
37. Andriole G, Lieber M, Smith J, Soloway M, Schroeder F, Kadmon D, DeKernion J, Rajfer J, Boake R, Crawford D, et al. Treatment with finasteride following radical prostatectomy for prostate cancer. *Urology*. 1995 Mar;45(3):491-7. PubMed PMID: 7533461.
38. Oh WK, Manola J, Bittmann L, Brufsky A, Kaplan ID, Smith MR, Kaufman DS, Kantoff PW. Finasteride and flutamide therapy in patients with advanced prostate cancer: response to subsequent castration and long-term follow-up. *Urology*. 2003 Jul;62(1):99-104. PubMed PMID: 12837431.
39. Eggener SE, Stern JA, Jain PM, Oram S, Ai J, Cai X, Roehl KA, Wang Z. Enhancement of intermittent androgen ablation by "off-cycle" maintenance with finasteride in LNCaP prostate cancer xenograft model. *The Prostate*. 2006 Apr 1;66(5):495-502. PubMed PMID: 16372330.

40. Scholz MC, Jennrich RI, Strum SB, Johnson HJ, Guess BW, Lam RY. Intermittent use of testosterone inactivating pharmaceuticals using finasteride prolongs the time off period. *J Urology*. 2006 May;175(5):1673-8. PubMed PMID: WOS:000236928400019. English.
41. Sartor O, Nakabayashi M, Taplin ME, Ross RW, Kantoff PW, Balk SP, Oh WK. Activity of dutasteride plus ketoconazole in castration-refractory prostate cancer after progression on ketoconazole alone. *Clinical genitourinary cancer*. 2009 Oct;7(3):E90-2. PubMed PMID: 19815488.
42. Shah SK, Trump DL, Sartor O, Tan W, Wilding GE, Mohler JL. Phase II study of Dutasteride for recurrent prostate cancer during androgen deprivation therapy. *The Journal of urology*. 2009 Feb;181(2):621-6. PubMed PMID: 19091347. Pubmed Central PMCID: 2851185.
43. Taplin ME, Regan MM, Ko YJ, Bubley GJ, Duggan SE, Werner L, Beer TM, Ryan CW, Mathew P, Tu SM, Denmeade SR, Oh WK, Sartor O, Mantzoros CS, Rittmaster R, Kantoff PW, Balk SP. Phase II Study of Androgen Synthesis Inhibition with Ketoconazole, Hydrocortisone, and Dutasteride in Asymptomatic Castration-Resistant Prostate Cancer. *Clinical Cancer Research*. 2009 Nov 15;15(22):7099-105. PubMed PMID: WOS:000271822600043. English.
44. Hamid AR, Verhaegh GW, Smit FP, van Rijt-van de Westerlo C, Armandari I, Brandt A, Sweep FC, Sedelaar JP, Schalken JA. Dutasteride and enzalutamide synergistically suppress prostate tumor cell proliferation. *The Journal of urology*. 2015 Mar;193(3):1023-9. PubMed PMID: 25242390.
45. Cantagrel V, Lefeber DJ, Ng BG, Guan Z, Silhavy JL, Bielas SL, Lehle L, Hombauer H, Adamowicz M, Swiezewska E, De Brouwer AP, Blumel P, Sykut-Cegielska J, Houliston S, Swistun D, Ali BR, Dobyns WB, Babovic-Vuksanovic D, van Bokhoven H, Wevers RA, Raetz CR, Freeze HH, Morava E, Al-Gazali L, Gleeson JG. SRD5A3 is required for converting

polyprenol to dolichol and is mutated in a congenital glycosylation disorder. *Cell*. 2010 Jul 23;142(2):203-17. PubMed PMID: 20637498. Pubmed Central PMCID: 2940322.

46. Stiles AR, Russell DW. SRD5A3: A surprising role in glycosylation. *Cell*. 2010 Jul 23;142(2):196-8. PubMed PMID: 20655462. Pubmed Central PMCID: 3104503.

47. Kahrizi K, Hu CH, Garshasbi M, Abedini SS, Ghadami S, Kariminejad R, Ullmann R, Chen W, Ropers HH, Kuss AW, Najmabadi H, Tzschach A. Next generation sequencing in a family with autosomal recessive Kahrizi syndrome (OMIM 612713) reveals a homozygous frameshift mutation in SRD5A3. *European journal of human genetics : EJHG*. 2011 Jan;19(1):115-7. PubMed PMID: 20700148. Pubmed Central PMCID: 3039499.

48. Morava E, Wevers RA, Cantagrel V, Hoefsloot LH, Al-Gazali L, Schoots J, van Rooij A, Huijben K, van Ravenswaaij-Arts CM, Jongmans MC, Sykut-Cegielska J, Hoffmann GF, Bluemel P, Adamowicz M, van Reeuwijk J, Ng BG, Bergman JE, van Bokhoven H, Korner C, Babovic-Vuksanovic D, Willemsen MA, Gleeson JG, Lehle L, de Brouwer AP, Lefeber DJ. A novel cerebello-ocular syndrome with abnormal glycosylation due to abnormalities in dolichol metabolism. *Brain : a journal of neurology*. 2010 Nov;133(11):3210-20. PubMed PMID: 20852264.

49. Godoy A, Kawinski E, Li Y, Oka D, Alexiev B, Azzouni F, Titus MA, Mohler JL. 5alpha-reductase type 3 expression in human benign and malignant tissues: a comparative analysis during prostate cancer progression. *The Prostate*. 2011 Jul;71(10):1033-46. PubMed PMID: 21557268. Pubmed Central PMCID: 4295561.

50. Yamana K, Labrie F, Luu-The V. Human type 3 5alpha-reductase is expressed in peripheral tissues at higher levels than types 1 and 2 and its activity is potently inhibited by

finasteride and dutasteride. *Hormone molecular biology and clinical investigation*. 2010 Aug 1;2(3):293-9. PubMed PMID: 25961201.

51. Titus MA, Li Y, Kozyreva OG, Maher V, Godoy A, Smith GJ, Mohler JL. 5alpha-reductase type 3 enzyme in benign and malignant prostate. *The Prostate*. 2014 Feb;74(3):235-49. PubMed PMID: 24150795. Pubmed Central PMCID: 3992828.

52. Chavez B, Ramos L, Garcia-Becerra R, Vilchis F. Hamster SRD5A3 lacks steroid 5alpha-reductase activity in vitro. *Steroids*. 2015 Feb;94:41-50. PubMed PMID: 25498908.

53. Luu-The V. Assessment of steroidogenesis and steroidogenic enzyme functions. *The Journal of steroid biochemistry and molecular biology*. 2013 Sep;137:176-82. PubMed PMID: 23770321.

54. Loblaw DA, Virgo KS, Nam R, Somerfield MR, Ben-Josef E, Mendelson DS, Middleton R, Sharp SA, Smith TJ, Talcott J, Taplin M, Vogelzang NJ, Wade JL, 3rd, Bennett CL, Scher HI, American Society of Clinical O. Initial hormonal management of androgen-sensitive metastatic, recurrent, or progressive prostate cancer: 2006 update of an American Society of Clinical Oncology practice guideline. *Journal of clinical oncology : official journal of the American Society of Clinical Oncology*. 2007 Apr 20;25(12):1596-605. PubMed PMID: 17404365.

55. Aggarwal S, Thareja S, Verma A, Bhardwaj TR, Kumar M. An overview on 5alpha-reductase inhibitors. *Steroids*. 2010 Feb;75(2):109-53. PubMed PMID: 19879888.

56. Montgomery RB, Mostaghel EA, Vessella R, Hess DL, Kalhorn TF, Higano CS, True LD, Nelson PS. Maintenance of intratumoral androgens in metastatic prostate cancer: a mechanism for castration-resistant tumor growth. *Cancer research*. 2008 Jun 1;68(11):4447-54. PubMed PMID: 18519708. Pubmed Central PMCID: 2536685.

57. Storbeck KH, Bloem LM, Africander D, Schloms L, Swart P, Swart AC. 11beta-Hydroxydihydrotestosterone and 11-ketodihydrotestosterone, novel C19 steroids with androgenic activity: a putative role in castration resistant prostate cancer? *Molecular and cellular endocrinology*. 2013 Sep 5;377(1-2):135-46. PubMed PMID: 23856005.

## VITA

Zahi I Mitri was born on June 17<sup>th</sup>, 1985 to Ibrahim Najib Mitri and Gisele Assi Mitri. After graduating from Athenee de Beyrouth high school in Bsalim, Lebanon in 2003, Zahi enrolled at The American University of Beirut where he completed his undergraduate and medical degrees. Zahi graduated with a bachelor of science in biology from The American University of Beirut in 2006. Following that, he enrolled in The American University of Beirut Medical School and graduated in 2010. After graduation, Zahi joined the Internal Medicine Residency Program at Emory University Hospital in Atlanta, Georgia. He completed his internal medicine degree in 2013, following which he was accepted to join the Hematology and Medical Oncology Fellowship at The University of Texas MD Anderson Cancer Center. He is expected to graduate from his fellowship program in June of 2016. He began his work in the University Of Texas Graduate School Of Biomedical Sciences in the fall of 2014, under the mentorship of Dr. Mark Titus, Ph.D. Zahi has accepted a faculty position at The Oregon Health and Science University at the completion of his training program. He will work as an assistant professor at the Knight Cancer Institute, with a focus in breast medical oncology.